



Autism gene Ube3a and seizures impair sociability by repressing VTA Cbln1

The Harvard community has made this article openly available. [Please share](#) how this access benefits you. Your story matters

Citation	Krishnan, V., D. C. Stoppel, Y. Nong, M. A. Johnson, M. J. Nadler, E. Ozkaynak, B. L. Teng, et al. 2017. "Autism gene Ube3a and seizures impair sociability by repressing VTA Cbln1." Nature 543 (7646): 507-512. doi:10.1038/nature21678. http://dx.doi.org/10.1038/nature21678 .
Published Version	doi:10.1038/nature21678
Citable link	http://nrs.harvard.edu/urn-3:HUL.InstRepos:34491817
Terms of Use	This article was downloaded from Harvard University's DASH repository, and is made available under the terms and conditions applicable to Other Posted Material, as set forth at http://nrs.harvard.edu/urn-3:HUL.InstRepos:dash.current.terms-of-use#LAA



Published in final edited form as:

Nature. 2017 March 23; 543(7646): 507–512. doi:10.1038/nature21678.

Autism gene *Ube3a* and seizures impair sociability by repressing VTA *Cbln1*

Vaishnav Krishnan^{*1}, David C. Stoppel^{*1,2,7}, Yi Nong^{*1,2}, Mark A. Johnson^{1,2}, Monica J.S. Nadler^{1,2}, Ekim Ozkaynak^{1,2}, Brian L. Teng^{1,2}, Ikue Nagakura^{1,2}, Fahim Mohammad², Michael A. Silva^{1,2}, Sally Peterson^{1,2}, Tristan J. Cruz^{1,2}, Ekkehard M. Kasper³, Ramy Arnaout^{2,4,5}, and Matthew P. Anderson^{‡,1,2,6,7}

¹Department of Neurology, Beth Israel Deaconess Medical Center, 330 Brookline Avenue, Boston, MA 02115, USA

²Department of Pathology, Beth Israel Deaconess Medical Center, 330 Brookline Avenue, Boston, MA 02115, USA

³Department of Surgery, Beth Israel Deaconess Medical Center, 330 Brookline Avenue, Boston, MA 02115, USA

⁴Division of Clinical Informatics, Department of Internal Medicine, Beth Israel Deaconess Medical Center, 330 Brookline Avenue, Boston, MA 02215, USA

⁵Department of Systems Biology, Harvard Medical School, Boston, MA 02115, USA

⁶Boston Children's Hospital Intellectual and Developmental Disabilities Research Center, 300 Longwood Avenue, Boston, MA 02115, USA

⁷Program in Neuroscience, Harvard Medical School, 300 Longwood Avenue, Boston, MA 02115, USA

Summary

Maternally inherited 15q11-13 chromosomal triplications cause a frequent and highly penetrant autism linked to increased gene dosages of *UBE3A*, which both possesses ubiquitin-ligase and transcriptional co-regulatory functions. Here, using *in vivo* mouse genetics, we show that increasing *UBE3A* in the nucleus down-regulates glutamatergic synapse organizer cerebellin-1

Users may view, print, copy, and download text and data-mine the content in such documents, for the purposes of academic research, subject always to the full Conditions of use: http://www.nature.com/authors/editorial_policies/license.html#terms

[‡]To whom correspondence should be addressed: Matthew P. Anderson, MD, PhD, Associate Professor, Harvard Medical School, Faculty, Program in Neuroscience, Harvard Medical School, Director of Neuropathology, Department of Pathology, Beth Israel Deaconess Medical Center, Director (Boston Node) and Neuropathologist, Autism BrainNET, Investigator, Boston Children's Hospital Intellectual and Developmental Disabilities Research Center; Center for Life Science, 330 Brookline Ave, E/CLS-645, Boston, MA 02215, Tel: (617) 735-3202, FAX: (617) 735-3249, Matthew_Anderson@bidmc.harvard.edu, www.hms.harvard.edu/dms/neuroscience/fac/Anderson.html.

*These authors contributed equally to this work.

Competing Financial Interests: The authors report no competing financial or other conflicts of interest.

Author Contributions: V.K., D.C.S., Y.N., and M.P.A. designed the study. V.K. and M.P.A. wrote the manuscript. V.K., D.C.S. and Y.N. performed all experiments and analyses except for the following: E.O., M.N. and T.J.C. validated microarray-identified gene regulations by qRT-PCR; F.M. and R.A. and M.P.A. performed gene ontology and cluster visualization; I.N. performed nuclear/cytosolic fractionation studies; S.P. performed olfaction and open field experiments; M.A.J., B.T., M.S., E.M.K., and M.N. developed molecular probes and constructs.

(*Cbln1*) that is needed for sociability in mice. Epileptic seizures also repress *Cbln1* and are found to expose sociability impairments in mice with asymptomatic increases of UBE3A. This *Ube3a*-seizure synergy maps to glutamate neurons of the midbrain ventral tegmental area (VTA) where *Cbln1* deletions impair sociability and weaken glutamatergic transmission. We provide preclinical evidence that viral-vector-based chemogenetic activations of, or *Cbln1* restorations in VTA glutamatergic neurons rescues sociability deficits induced by *Ube3a* and/or seizures. Our results suggest a *gene* × *seizure* interaction in VTA glutamatergic neurons that impairs sociability by downregulating *Cbln1*, a key node in the expanding protein interaction network of autism genes.

Diverse genetic defects, immunological insults, and certain epilepsies have been implicated in the pathophysiology of autism spectrum disorder (ASD)^{1,2}. These varied etiologies may converge to disrupt specific molecular interactions in specialized neuronal subtypes to produce autism's sociability deficits. A common and highly penetrant genetic ASD results from maternally inherited 15q11-13 *triplications*^{3,4} that triples the neuron-expressed gene dosage of *UBE3A*, which is deleted in Angelman syndrome⁵⁻⁸. *UBE3A* encodes a dual-function E3 ubiquitin ligase⁹ and transcriptional co-regulator¹⁰. We previously demonstrated that mice with increased genomic *Ube3a* copies ("Ube3a2x" mice) display impaired sociability, diminished conspecific ultrasonic vocalizations and heightened repetitive self-grooming, together with deficits in cortical excitatory transmission⁴. However, the subcellular locus, downstream molecular mechanisms and circuit deficits responsible for UBE3A's impact on sociability remain unknown.

UBE3A effects map to the nucleus

To address these questions, we first examined the altered cortical transcriptional landscape in Ube3a2x mice which display a ~3 fold increase in total UBE3A protein^{4,11}. On an Affymetrix microarray analysis of total RNA from whole cortex of adult Ube3a2x and wild type (WT) littermate mice, we identified 190 up- and 408 down-regulated genes (p<0.05 FDR adjusted, ±1.4 fold cutoff, Supplementary Table 1), enriched for glutamatergic synaptic transmission function (Supplementary Table 2). To understand how they interact with known ASD genes, we visualized (Fig. 1a, Extended Data Fig. 1) how their encoded proteins are positioned within a network of protein-protein physical interactions with 276 genes strongly implicated in autism¹² (Supplementary Table 3). As a candidate downstream mediator of UBE3A's effects, we focused on *Cerebellin-1* (*CBLN1*) because it was dose-dependently repressed by UBE3A and binds presynaptic NRXN1/2/3 and postsynaptic GRID1/2¹³⁻¹⁷, two gene families deleted or mutated in ASD^{3,12}. NRXN-CBLN1-GRID trimolecular complexes trans-synaptically organize glutamatergic synapse formation¹⁶⁻¹⁹. *Cbln1* also compensates for congenital losses of *Cbln3*²⁰. With quantitative real-time PCR, we found *Cbln1* downregulations in cortical samples from Ube3a1x and Ube3a2x mice (heterozygous or homozygous for a C-terminal FLAG-tagged *Ube3a* transgene⁴, respectively). *Cbln1* was also repressed in "Ube3aNLS" mice (heterozygous for a FLAG-tagged UBE3A confined to the nucleus with two nuclear localization signals, Extended Data Fig. 2a-d) and in Ube3a2x (untagged) mice (homozygous for an untagged *Ube3a* gene) (Fig. 1b). Cortical *Cbln1* expression was elevated in *hemizygous* Ube3a^{mKO} mice (modeling Angelman syndrome)⁵, whether the deleted *Ube3a* allele was inherited from an "asymptomatic" mother (*paternally*-

deleted allele, “p-Ube3a^{mKO}”) or “affected” mother (*maternally*-deleted allele, “m-Ube3a^{mKO}”) ²¹. Several UBE3A down-regulated genes displayed dose-dependent and nuclear-mediated effects (Fig. 1c, Extended Data Fig. 3), a finding less consistent for UBE3A up-regulated genes (Extended Data Fig. 4).

Transgenic increases of *Ube3a* also impacted conspecific social behavior in a dose-dependent manner (irrespective of the presence of a C-terminal tag). However, this dose dependence was overcome by targeting UBE3A to the nucleus. In the three chamber sociability task ²² (see Methods), Ube3a2x mice ⁴ as well as Ube3a2x (untagged) mice displayed impaired sociability (Fig. 1d, Extended Data Fig. 2e,f). Two independent Ube3aNLS lines (lines “3” and “7”) also displayed impaired sociability. In contrast, sociability was not repressed in Ube3a1x or Ube3a^{mKO} mice. Ube3a2x (untagged) and Ube3aNLS mice also emitted fewer ultrasonic vocalizations (USVs) (Fig. 1e) and displayed fewer physical interactions when exposed to genotype-matched strangers (Extended Data Fig. 2g). These social phenotypes could not be explained by changes in grooming, olfaction, exploration or locomotion (Extended Data Fig. 2h–m). Therefore, an otherwise asymptomatic increase of UBE3A (Extended Data Fig. 2a), when confined to the nucleus (in Ube3aNLS mice), recapitulates the transcriptional downregulations and impaired sociability seen in Ube3a2x mice.

To directly connect decreased *Cbln1* expression to impaired sociability, we deleted *Cbln1* in glutamatergic *VGluT2*⁺ (vesicular glutamate transporter type 2) neurons. *VGluT2*Cre.*Cbln1*^{fl/fl} mice had reduced *Cbln1* expression across several brain regions (Fig. 1f, Extended Data Fig. 5a), impaired sociability (Fig. 1g, Extended Data Fig. 5b,c), and fewer USVs and physical interactions with stranger females (Fig. 1h, Extended Data Fig. 5d). Grooming, exploration, locomotion and olfaction were unaffected, although rotarod performance was mildly impaired (Extended Data Fig. 5e–k). Thus, deleting *Cbln1* in *VGluT2*Cre-labeled neurons reconstitutes the social deficits of Ube3a2x (tagged or untagged) and Ube3aNLS mice. Together with the reported sociability impairments in homozygous *Grid1*KO mice ²³, these results implicate glutamate synapses dependent on CBLN1 and GRID1 in promoting normal sociability.

Seizure-induced deficits are UBE3A-dependent

Cbln1 mRNA is also repressed by increased neuronal activity in cerebellum in culture after depolarization and *in vivo* after status epilepticus ²⁴. Therefore, we tested whether recurrent seizures can concurrently repress *Cbln1* and sociability. We exposed WT mice to 10 successive daily injections of GABA antagonist pentylentetrazole (PTZ) at subconvulsant doses (30 mg/kg) and observed a gradual increase in seizure severity (Fig. 2a left, Extended Data Fig. 6a,b). 24h later, *Cbln1* mRNA was repressed in several brain regions (Fig. 2a right), sociability was impaired ²⁵ and social USVs were reduced (Fig. 2b,c) without impacting exploration, locomotion, grooming or olfaction (Extended Data Fig. 6c–k). This sociability deficit persisted for 30 days (Extended Data Fig. 6l,m). To examine how *Ube3a* dosage might impact seizure-induced social impairments, we applied 10 PTZ-induced seizures to p-Ube3a^{mKO}, m-Ube3a^{mKO} and their corresponding WT littermates. Seizure severities were similar, but both Ube3a^{mKO} mice were resistant to seizure-induced deficits in

sociability (Fig. 2d–g, Extended Data Fig. 6n). Conversely, to test if “asymptomatic” increases of UBE3A augment seizure-induced sociability deficits, we applied a “subthreshold” PTZ paradigm to *Ube3a*1x (untagged) mice where five 30 mg/kg PTZ injections are delivered *every other day*. 24h later, *Ube3a*1x (untagged) mice displayed impaired sociability whereas WT littermates were unaffected (Fig. 2h–j, Extended Data Fig. 6o,p). Seizure effects were not explained by changes in *Ube3a* mRNA (Extended Data Fig. 6q). Overall, these results demonstrate that UBE3A is necessary for seizure-induced decreases in sociability and *Cbln1* expression, and illustrate an *Ube3a*-seizure synergy in promoting impaired sociability.

UBE3A-seizure synergy maps to VTA

To identify the neuronal circuits underlying this synergy, we engineered our full-length *Ube3a-FLAG* construct⁴ with a *loxP*-flanked transcriptional/translational blocker (TB) cassette in intron 1. In these “LoxTBUbe3a” transgenic mice, cell-type specific *Cre* expression deletes the TB cassette to activate UBE3A-FLAG expression and moderately increase total *Ube3a* mRNA (Fig. 3a,b,f, Extended Data Fig. 7a–h). Baseline sociability was not impaired in mice with UBE3A-FLAG expression targeted by *VGluT2Cre*, *VGaTCre*, *EMXCre*, *Math1Cre*, *DATCre*, *DBHCre*, *ChATCre* or *ePetCre* driver lines (Fig. 3c,g, Extended Data Figs. 7c–h, 8). However, sociability deficits were produced by the “subthreshold” PTZ paradigm in mice with UBE3A-FLAG increased in *VGluT2* or *DAT* (dopamine transporter) expressing neurons (Fig. 3d,e,h,i, Extended Data Fig. 8). *DAT*⁺ and *VGluT2*⁺ neurons co-exist in the ventral tegmental area (VTA), alongside GABAergic and glutamate/dopamine co-releasing neurons^{26,27}. Optogenetic modulation of VTA dopaminergic projections to nucleus accumbens (NAc) alters social approach behavior in mice²⁸. VTA *VGluT2*⁺ neurons are situated in medial VTA²⁹ and project to several regions including NAc²⁶, but have not been ascribed a role in social behavior. Following 10 daily recurrent PTZ seizures, VTA *Cbln1* mRNA levels were elevated in *Ube3a*^{mKO} mice and repressed in *Ube3a*1x (untagged) mice (Fig. 2k, with similar results obtained in *Ube3a*1x⁴ mice, Extended Data Fig. 9a). Thus, changes in VTA *Cbln1* expression parallel the relative resistance of *Ube3a*^{mKO} and vulnerability of *Ube3a*1x (tagged or untagged) mice to seizure-induced sociability deficits.

To selectively increase untagged UBE3A in VTA *VGluT2*⁺ neurons, we injected the VTA of *VGluT2Cre* and WT littermate mice with AAV-hSyn-DIO-*Ube3a* (human isoform 3, enabling *Cre-recombinase* mediated expression of untagged *Ube3a*, Fig. 3j). Sociability was preserved at baseline, but impaired by the “subthreshold” PTZ paradigm (Fig. 3k–m, Extended Data Fig. 9b,c). Thus, increasing UBE3A selectively in VTA *VGluT2*⁺ neurons synergizes with seizures to impair sociability.

Midbrain VTA-targeted deletion of *Cbln1*

To link VTA *Cbln1* mRNA down-regulations to sociability deficits, we infused AAVCreGFP (or AAVGFP) into VTA of *Cbln1*^{fl/fl} mice. 20d later, Cre-injected mice displayed impaired sociability without changes in locomotion or exploration (Fig. 4a, Extended Data Fig. 9d–f). Similarly, mice with *VGluT2* neuron-targeted deletions of *Cbln1* in VTA displayed impaired

sociability (AAV-encoded *Cre*-RFP or RFP alone driven by the *VGluT2* promoter, 28d later; Fig. 4b, Extended Data Fig. 9g). These effects were cell-type specific in VTA: *Cbln1* deletions restricted to *DAT*⁺ neurons did not impair sociability (Fig. 4c, Extended Data Fig. 9h). Given *Cbln1*'s role in the integrity of cerebellar glutamatergic synapses^{14,28}, we tested whether *Cbln1* deletions in VTA or recurrent seizures impair glutamatergic transmission. We deleted VTA *Cbln1* by injecting AAVCreGFP into VTA of *Cbln1*^{fl/fl} mice harboring a *Cre*-inducible form of a light-activated excitatory opsin (*Channelrhodopsin-2*, *ChR2*, ChR2-EYFP or “Ai32” mice), enabling light-induced excitation of axon terminals in VTA targets (Fig. 4d). 6 weeks later, patch-clamp recordings from medium spiny neurons (MSN) in NAc medial shell (a VTA glutamatergic neuron target²⁶), with GABA_A receptor antagonist bicuculline present revealed that VTA *Cbln1* deletion or the experience of 10 PTZ-induced seizures strongly reduces light-evoked excitatory post-synaptic currents (EPSCs, Fig. 4e, Extended Data Fig. 9i–l). The frequency of spontaneous EPSCs in NAc medial shell MSNs was also decreased (Fig. 4f, Extended Data Fig. 9i). To examine glutamatergic transmission specifically from VTA *VGluT2*⁺ neurons, we injected AAV-DIO-ChR2-EYFP into the VTA of *VGluT2*Cre.*Cbln1*^{fl/fl} and *VGluT2*Cre mice. 30d later, *VGluT2*-specific *Cbln1* deletion also repressed these light-evoked EPSCs in NAc (Fig. 4g,h).

VTA glutamate neurons drive sociability

These results suggested that reducing VTA glutamatergic transmission might itself impair sociability. We selectively deleted *VGluT2* in VTA by injecting AAVCreGFP (or AAVGFP) into *VGluT2*^{fl/fl} mice. 20 days later, VTA-targeted *VGluT2* deletions impaired sociability without affecting locomotion or exploration (Fig. 4i, Extended Data Fig. 9m–o). Again, these effects were cell-type specific: *VGluT2* deletion in *DAT*⁺ neurons did not impair sociability (Fig. 4j, Extended Data Fig. 9p). Thus, a viral-mediated or seizure-induced loss of *Cbln1* in VTA *VGluT2*⁺ neurons impairs VTA glutamatergic synaptic transmission that is necessary for normal sociability.

To interrogate how acutely regulating VTA *VGluT2*⁺ neuron activity impacts sociability, we applied chemogenetics approaches. *VGluT2*Cre mice received VTA injections of AAV-DIO-HA-KORD-IRES-citrine, permitting *Cre*-dependent expression of an inhibitory Gi-coupled designer receptor activated by Salvinorin-B [SALB]. 28d later, subcutaneous administration of SALB acutely repressed sociability (Fig. 5a, Extended Data Fig. 10a). Conversely, to acutely increase VTA *VGluT2*⁺ neuron activity, *VGluT2*Cre mice were injected with AAV-DIO-hM3D(Gq)-mCherry in the VTA, enabling the expression of an excitatory Gq-coupled designer receptor activated by clozapine-N-oxide (CNO). 28d later, intraperitoneal CNO administration acutely increased sociability in seizure-naïve mice (persisting through a *second* 5 minutes of a “social trial”, Fig. 5b, Extended Data Fig. 10b).

Rescuing sociability deficits

Acute chemogenetic activation of VTA *VGluT2*⁺ neurons also therapeutically restored sociability in mice with deficits produced by the *Ube3a*-seizure synergy or by ten PTZ-induced seizures (Fig. 5c,d, Extended Data Fig. 10c,d). *VGluT2*Cre mice were co-injected with AAV-hSyn-DIO-Ube3a *and* either AAV-DIO-GFP or AAV-hSyn-DIO-Cbln1-IRES-

RFP. Increased *Cbln1* expression in VTA *VGlut2+* neurons did not affect baseline social behavior or seizure severity scores, but did protect against the sociability deficits produced by the UBE3A seizure synergy (Fig. 5e–g, Extended Data Fig. 10e). These results indicate that diminished *Cbln1* expression in VTA *VGlut2+* neurons plays a critical pathogenic role in mediating the effects of seizures and increased *Ube3a* on sociability.

Discussion

Our results suggest that UBE3A increases found in 15q11-13 ASD patients¹¹ may repress *CBLN1* expression to disrupt NRXN-CBLN1-GRID1 complexes and compromise glutamatergic synaptic transmission. This mechanism may also contribute to social impairments in patients with biologically-related genetic defects (e.g., *GRID1* or *NRXN1* deletions) and other ASD patients with comorbid seizures². We show that neuronal UBE3A is necessary for seizure-induced *Cbln1* repression, potentially functioning as a transducer of pathologic activity-induced changes in gene expression³⁰. UBE3A may repress *Cbln1* through its transcriptional co-regulatory functions^{10,31,32}. For example, UBE3A physically interacts with MECP2³³ (methyl CpG-binding protein 2, deleted in Rett syndrome) that represses a subset of genes through interactions with the NCoR repressor complex (nuclear receptor co-repressor)³⁴. Seizures upregulate the transcriptional repressor REST (RE-1 silencing transcription factor) in hippocampus^{35,36} as well as in VTA (Extended Data Fig. 10f), and *Cbln1* intron 2 contains a consensus RE-1 that binds REST³⁷ (Extended Data Fig. 10g). Seizures may also enhance UBE3A's transcriptional modulatory functions by dephosphorylating threonine 480 (T485 in humans) to promote nuclear translocation³⁸. Indeed, our behavioral and molecular findings in Ube3aNLS mice support such a model. With native UBE3A still present and the potential to homomultimerize³⁹, our experimental approach does not exclude a role of UBE3A's E3-ligase functions^{9,38,40}. Increased UBE3A was found to amplify the detrimental effects of seizures on sociability, an effect localized to VTA glutamatergic neurons where *Cbln1* repression plays a major role. Importantly, restoring *Cbln1* expression in these neurons was sufficient to therapeutically rescue impaired sociability. Seizures also synergized with increased UBE3A in dopaminergic neurons, likely occurring through *Cbln1*-independent mechanisms^{41,42}. Overall, these findings establish that VTA glutamatergic neurons drive sociability, and implicate *Cbln1* downregulations within these neurons as a critical convergence point in the pathogenesis of sociability deficits in a genetic form of autism with epilepsy comorbidity.

Methods

Mice

The Harvard Medical Area Standing Committee on Animals and the Institutional Animal Care and Use Committee of Beth Israel Deaconess Medical Center approved all mouse protocols. Mice were housed at the Center for Life Sciences barrier animal facility in sex-matched groups of 3–5 with ad libitum food (except for olfaction testing) and water access. Lights were on between 0700 and 1900hrs when behavioral testing/seizure induction was performed. Unless otherwise specified, littermate controls were used and cohorts were a mixture of male and female mice at a ratio of approximately 1:1. For experiments involving

PTZ/saline injections in WT mice (e.g., Fig. 2a–c), separate cohorts of WT FVB mice were bred within our colony. Ube3a transgenic mice were generated using bacterial artificial chromosome (BAC) recombineering techniques as described previously^{4,43,44}. For Ube3aNLS mice, three FLAG tags were added to the C-terminal end of this construct followed by two in-frame nuclear localization signals from the SV40 large antigen, followed by two stop codons. For LoxTBUbe3a mice, a loxP-flanked transcriptional blocker cassette (containing the *Engrailed 2* splice acceptor followed by a poly-A tail and a neomycin resistance positive selection marker⁴⁵) was introduced into intron 1 of the C-terminal triple-FLAG tagged *Ube3a* to block expression of all splice variants of *Ube3a*. For experiments in Fig. 3a–i and Extended Data Fig. 7,8, LoxTBUbe3a mice were bred to homozygosity. Since there is evidence that C-terminal extensions/modifications of UBE3A are detrimental to ubiquitin ligase activity against certain targets^{32,46}, we also generated Ube3a1x (untagged) mice with a full length *Ube3a* construct that is unmodified. BAC DNA was prepared using a Nucleobond BAC maxi-preparation kit (Clontech) and validated by sequencing analysis. Constructs were linearized and microinjected into FVB/NJ embryos at the BIDMC Transgenic Core Facility. Male and female (tagged⁴ or untagged) Ube3a1x mice were crossed to result in WT, Ube3a1x and Ube3a2x mice. To determine transgenic Ube3a copy number, genomic DNA was isolated from mouse tail clips using the Purelink Genomic DNA Mini Kit (ThermoFisher). Real-time quantitative PCR was performed to measure genomic copies of *Ube3a* and *Tfrc* (transferrin receptor) using Taqman® Mm00238405_cn probe (Ube3a) and Taqman® Copy Number Reference Assay (Tfrc) with Taqman® Genotyping Master Mix (ThermoFisher). Absolute *Ube3a* copy number was calculated using the $2^{-(C_T)}$ method and multiplying by a factor of two (two *Tfrc* alleles). This technique revealed the following approximate total copy numbers (i.e., including the two native Ube3a copies): Ube3a2x (7.8 ± 0.4 , n=4), LoxTBUbe3a (8.97 ± 0.16 , n=5), Ube3a2x untagged (5.13 ± 0.15 , n=8), Ube3aNLS7 (3.59 ± 0.13 , n=6). Ube3a^{mKO} mice⁵ (Jackson Labs) were backcrossed 9 generations to FVB/NJ before behavioral testing. Both p-Ube3a^{mKO} and m-Ube3a^{mKO} mice were generated based on the breeding scheme described in Fig. 1b. The following lines were bred into an FVB/NJ genetic background for 6 or more generations. Cbln1^{fl/fl} mice¹⁷ were a generous gift from Dr. Masayoshi Mishina (Nigata University, Tokyo, Japan). VGluT2Cre⁴⁷ mice and VGaTCre mice⁴⁷ were provided as a generous gift from Dr. Bradford Lowell (BIDMC). VGluT2^{fl/fl}⁴⁸, EMX-Ires-Cre⁴⁹, Math1Cre⁵⁰, DATCre⁵¹, DBHCre⁵², ChATCre⁵³, ePETCre⁵⁴, and Ai32//ChR2-EYFP⁵⁵ lines of mice were purchased from Jackson Labs.

Tissue

Brains were rapidly removed and submerged in ice-cold phosphate buffered saline (PBS) for 20–30s. For the isolation of cortex (microarray and validation studies), two “slabs” of total cortex were dissected using curved forceps. For tissue punches, the PBS-cooled brain was placed in a brain matrix (ASI Instruments) and razor blades were placed at 1mm intervals to obtain brain slices. For hippocampal specimens, the entire hippocampal formation from one slice was carefully dissected so as to include all subfields. Punches were obtained with a 1mm (retrosplenial cortex, cerebellum) or a 0.5 mm (rest) punch core needle (Harris Unicore, Extended Data Fig. 5a) and immediately frozen to –20 C and stored at –80 C.

RNA isolation, Affymetrix gene chip hybridization, and quantitative real time PCR (qRT-PCR)

RNA was isolated using Trizol Reagent (Invitrogen) and column-purified using the RNAeasy Protect Mini Kit (Qiagen). First strand cDNA synthesis was carried out with oligo-dTs and reverse transcriptase (Ambion). Microarray samples were hybridized to an Affymetrix GeneChip HT MG-430 PM array with tissue from six biological replicates of each genotype (WT and Ube3a2x) pooled into three pairs. Array normalization, expression value calculation and clustering analysis were performed using dChip software (www.dchip.org). We adjusted the statistical significance (nominal p-value) of the entire gene set to account for multiple testing by estimating the False Discovery rate (FDR). While estimating FDRs, we used 50 random permutations to obtain a final list of 597 probes that satisfied our assumed significance threshold of 0.05. Primer pairs were selected through Primer3⁵⁶ with specificity confirmed with Primer-BLAST⁵⁷. Melt-curve analysis and agarose gel electrophoresis were used to confirm a single PCR product of the appropriate amplicon size. For microarray validation, 3 separate cDNA samples (each combined from two independent biological samples) were amplified through qRT-PCR in triplicate using Sybr-Green (Life Technologies) on a BioRad CFX384 Real Time Thermal Cycler. Gene expression fold changes were calculated with the comparative CT method⁵⁸ and normalized to *GAPDH*, with similar results obtained normalizing to *RPLP0* (ribosomal protein, large, P0) or *POLR2a* (RNA polymerase II subunit A). Error bars for all qRT-PCR experiments are an upper error limit that represents a standard error of the mean for technical replicates from each sample, were calculated as follows: upper error = $2^{-(\text{average CT})} + [(\text{average}(\text{SD}_{\text{gene of interest}}^2 + \text{SD}_{\text{reference gene}}^2)^{1/2}/(\text{sample size})^{1/2})]$. Primer sequences are in Supplementary Table 4.

Gene annotations and protein interactions

Regulated genes were annotated according to Gene Ontology (GO). P-values for enrichment of each GO category were calculated using the Category, GOSTats, and KEGGREST packages of Bioconductor^{59,60} (Supplementary Table 2). 598 up- and down- regulated genes in Ube3a2x mice as well as SFARI (Simons Foundation Autism Research Initiative) genes identified as strongly implicated in autism¹² were used to build an initial physical protein-protein interaction network by searching seven current, high-quality, human-curated protein interaction networks [BioGRID, DIP (Database of Interacting Proteins), HPRD (Human Protein Reference Database), InnateDB, IntAct, MatrixDB, and MINT (Molecular Interaction Database)]. We searched for and displayed clusters of interactions between protein products of pairs of *Ube3a*-regulated genes, *Ube3a*-regulated and autism genes, or between autism genes. To reduce network complexity, gene nodes with edges connecting to a more select set of 276 SFARI genes with the strongest genetic evidence for a causal role in autism were included in the final network (Supplementary Table 3). We clustered and visualized the interactions using Cytoscape 3.2.0 and its GLay community clustering algorithm⁶¹.

Subcellular fractionation and western blotting

Nuclear and cytosolic fractions of cortical samples (Extended Data Fig. 2d) were separated using a commercially available reagent-based technique (Fisher Scientific) according to manufacturer instructions. Proteins were loaded onto 4–15% polyacrylamide gels (Bio-Rad), transferred to PVDF membranes, blocked with 5% nonfat milk in TBS-T, and incubated overnight at 4 degrees with the following antibodies; anti-Ube3a (#7526, Cell Signaling), anti-alpha-Tubulin (#3873, Cell Signaling), and anti-TATA-binding protein (TBP; #8515, Cell Signaling). After TBS-T washes, blots were incubated with species-specific HRP-conjugated secondary antibodies for 1–2 hours at room temperature. Blots were developed with Pico chemiluminescent reagent (Pierce) and digital images were acquired using the gel dock system (Bio-Rad). Following subcellular fractionation, nuclear and cytosolic Ube3a levels were normalized to levels of TBP and alpha-Tubulin, respectively.

Immunofluorescence

Mice were anesthetized with an intraperitoneal injection of tribromoethanol and then perfused with ice-cold PBS followed by cold 4% paraformaldehyde. Brains were cryoprotected in 15% sucrose and then 30% sucrose (each for 24 h) and then frozen in optical cutting temperature compound (Fisher Health Care). 16µm sections were cut on a cryostat and slide-mounted. When an anti-mouse secondary antibody was used, sections were blocked with MOM reagent (Vector) and then with 10% normal goat serum with 1% BSA and 0.5% Triton X100 in PBS and incubated at room temperature overnight with antibody (anti-UBE3A [1:200, BD Biosciences], anti-PSD95 [1:200, Neuromab], anti-GFP [1:200, Abcam] or FITC-conjugated anti-FLAG [1:200, Sigma]) in blocking solution. Sections were washed and when required, incubated with Alexa-conjugated secondary antibodies (Invitrogen) for 3 hours at room temperature, and then mounted in Vectashield with DAPI (Vector). Fluorescent images were taken using a LSM510 confocal microscope (Zeiss) or the VS120-SL 5 Slide Scanner (Olympus) and “representative” images are representative of at least 3 mice per group. For quantitative immunofluorescence (Extended Data Fig. 2c), cortex-containing sections of each genotype (Ube3aNLS, Ube3a1x, Ube3a2x) were placed on the same slide. Sections were stained as above with FITC-conjugated FLAG primary antibody (Sigma). After incubation with primary antibody overnight, sections were mounted and imaged. FLAG-FITC staining intensity was quantified from 3 mice per genotype. Quantification of nuclear protein was done using Image J and twenty randomly chosen cells identified using the DAPI stain were quantified per image; 3 images per mouse were examined. Neuropil staining was quantified in the same manner but regions devoid of DAPI staining were selected.

Behavioral measurements

Mice were always tested at 7–11 weeks of age and were sexually naïve. For experiments testing the effects of viral manipulations on behavior, mice were randomly assigned into two groups matched for sex and age. For mice that received seizures (or saline injections), all testing was conducted 24h following the last injection (or 30 days later). Prior to testing, mice were acclimatized to a dedicated behavioral suite for one hour. Three-chamber testing was performed as previously described⁴. A clear acrylic box (50×100 cm) containing

dividers with 10×10 cm passageways was employed to create a three-chambered arena. Ethovision videotracking software (Noldus) was used with an overhead camera (Rainbow). Two small metal enclosures were placed in opposite corners (“left” or “right”). During the *acclimation trial* (5 minutes), mice were placed into the center of the arena and allowed to freely explore, following which they were removed and placed into a holding cage. A novel sex- and age-matched non-littermate WT mouse was placed in one of the two metal enclosures, with the side alternated between trials to cancel side bias. Then, during the *social trial* (5 minutes unless otherwise specified), the test mouse was reintroduced to the arena and allowed to freely explore. Between each mouse, the arena was wiped with Clidox-S. “Sniffing times” were collected live during the social trial by a blinded observer trained to record the duration that a test mouse spends physically interacting/sniffing the “social” or “opposite” enclosures. Videotracking was utilized to collect the total distance moved and “chamber times” (in left, middle and right chambers) during social and acclimation trials and was congruent with sniffing times (e.g., Fig. 1d/Extended Data Fig. 2e). Chamber times for the social trial for all three chamber experiments are provided in Supplementary Table 5. As described by Crawley^{22,62}, sociability is either *present/intact* or *absent/impaired*, and was formally defined as a significant preference to explore (or “sniff”) the social cue over the inanimate wire mesh cage by a post-hoc test following a two-way repeated measures ANOVA (see Statistics). In general, mice ambulated slightly shorter distances overall during the social trial (e.g., Extended Data Fig. 2f) although this was not always the case (e.g., Extended Data Fig., 5c). *Ube3a^{mKO}* mice ambulated shorter distances across both trials, consistent with previous reports of reduced locomotion⁶³. Distances for both acclimation and social trials for all three chamber experiments are provided in Supplementary Table 5. For studies involving AAV2-DIO-hM3D(Gq)-mCherry virus, approximately 28 days following AAV injections, mice received intraperitoneal injections of clozapine-N-oxide (CNO, Sigma) dissolved in sterile saline 10 minutes prior to three-chamber testing. To demonstrate *increased* sociability in naive mice (that display preserved baseline sociability), an additional 5 minutes long “social” trial was performed immediately after the first. For open field testing⁴, mice were placed into a 60×60 cm arena and freely explored for 10 minutes. Distance moved and the time spent in the center (a concentric 40×40 cm square) was measured by video tracking. For elevated plus maze testing (10 cm arm width, 30 cm wall elevation, 55 cm off the ground), mice freely explored for 10 minutes during which arm times and distances moved were measured by videotracking. For ultrasonic vocalization measurements⁴, pairs of adult mice were placed into a novel clean plastic container within a sound-isolated box for five minutes while the number of ultrasonic vocalizations were measured using the Ultravox System (Noldus) connected to Avisoft Pro software (Avisoft Bioacoustics). When pairs of females were tested, both mice were of the same genotype/treatment group (e.g., saline or PTZ) and age but never cage-mates. When male-female pairs were tested, test males were paired with independently bred WT age-matched sexually mature female mice. In certain experiments, simultaneous video-recordings were collected and blindly scored offline to obtain the total time spent physically interacting. The “buried food test” was employed to assay olfaction and was performed as described previously⁶⁴. For two consecutive days prior to testing, mice were exposed to a single Teddy Graham (Nabisco) within their home cage. Then, 24 h prior to testing, all food was removed from their home cages. On the test day, mice were individually placed into a fresh cage filled with

3cm of fresh bedding and a Teddy Graham buried in one randomly chosen corner. The time taken to find *and* begin to eat the Teddy Graham was recorded. For grooming measures, a blinded investigator live-scored the time spent grooming by a mouse placed into a fresh clean cage for 10 minutes⁴. Rotarod testing was performed on an accelerating rotarod (Ugo Basile) designed to accelerate from 4 to 40 rpm over five minutes. Mice were given three trials per day with a 60 minute inter-trial interval for three consecutive days. Fall latencies were obtained through an automated trip detector plate underneath each mouse. When multiple behavioral tests were performed on a single cohort of mice, the following order was strictly obeyed: three chamber sociability testing → ultrasonic vocalizations → grooming → open field testing / elevated plus maze testing → buried food testing → rotarod testing. No more than one test was performed on any given day.

Pentylentetrazole-induced seizures

Pentylentetrazole (Sigma) dissolved in 0.9% saline was injected intraperitoneally (10 ml/kg). Mice were then placed individually into fresh cages and no more than 3 mice were simultaneously observed for ten minutes by a trained blinded observer. Seizure severity was scored as previously described⁶⁵. Mice received a score of “1” when they displayed hypoactivity, defined as a decline in motor activity until the animal came to rest in a crouched or prone position with the abdomen in full contact with the cage bottom. A score of “2” was assigned if the animal displayed a single or multiple myoclonic jerks. Mice scored “3” when they displayed a generalized convulsion characterized by a sudden loss of upright posture with diffuse tonic posturing followed by clonic shaking. These episodes typically lasted between 20–40s, following which a prolonged period of hypoactivity was observed, occasionally interspersed with a few myoclonic jerks. Mice rarely achieved a score of “4”, defined as a similar generalized tonic clonic seizure with notable hind limb extension. These “maximal” convulsions typically preceded death, which across all experiments, occurred at a rate of no more than 0–20% per cohort (typically 0%). Mice never displayed more than one convulsion during the observation period. This PTZ protocol did not significantly impact general well-being, as reflected by their unimpaired weight gain (Extended Data Fig. 6b). Mice were assigned the “highest” score they achieved (i.e., a mouse that displayed hypoactivity together with myoclonic jerks scored “2”, whereas a mouse that displayed myoclonic jerks that progressed to a generalized convulsion scored “3”). While these scores are not continuous variables (and therefore strictly cannot be “averaged”), they nevertheless reflect a continuum of the behavioral responses to a PTZ injection. To provide a measure of the variability observed, each day’s average scores have been provided together with a standard error of the mean.

Stereotaxic surgery and viral vectors

Anesthesia was induced in a chamber with isoflurane/oxygen following which mice were placed into a stereotaxic frame fitted with a continuous isoflurane delivery system. A single midline vertical scalp incision revealed skull landmarks. Stereotaxic measurements were used to make 0.5mm wide burrholes over the entry point for bilateral viral injections directed at the VTA (0 deg, AP –3.3 mm, ML +/- 0.4 mm, DV –4.2 mm relative to bregma). 1 µl of virus was infused at 0.1µl/min through a 33gauge Hamilton needle connected to an automated infusion pump. Following each infusion, the needle remained in place for 5

minutes. The incision was sutured closed and a single injection of 10mg/kg meloxicam dissolved in saline was administered intraperitoneally for perioperative analgesia. All behavioral measurements were conducted approximately 20 days following surgery following which accurate targeting to the VTA was confirmed by immunohistochemistry. Electrophysiological assays were conducted at least 30 days after the surgery during which VTA sections were also examined for accurate placement. AAV2CreGFP, AAV2GFP, AAV2-DIO-GFP, AAV2-DIO-hM3D(Gq)-mCherry, and AAV2-EF1 α -Dio-hChR2(E123T/T159C)-EYFP were purchased from the University of North Carolina Viral Vector Core. For AAV-hSyn-DIO-Ube3a, the coding sequence of human Ube3a isoform 3 was amplified by PCR from Plasmid #37605 (Addgene) using primers to add a SpeI site to the 5' end and an AscI site to the 3' end. The resulting product was then ligated into NheI and AscI sites of the pAAV-hSyn-DIO-EGFP vector, Plasmid #50457 (Addgene). For AAV-hSyn-DIO-Cbln1-IRES-mCherry, the coding sequence of mouse Cbln1 was amplified from cDNA clone MGC:66947 IMAGE:6404555 using primers to add an XbaI site to the 5' end a BamHI site to the 3' end and was then subcloned into the pLVX-IRES-mCherry vector (Clontech). An MluI site 3' of mCherry was converted to an AscI site using the Q5[®] Site-Directed Mutagenesis Kit (New England Biolabs). The Cbln1-IRES-mCherry cassette was digested with XbaI and AscI and subcloned into NheI and AscI sites of the pAAV-hSyn-DIO-EGFP vector. To generate AAV-Vglut2-mCherry and AAV-Vglut2-mCherry-2A-Cre, the coding sequence of mCherry or mCherry-2A-Cre was amplified from pLM-CMV-R-Cre Plasmid #27546 (Addgene) with primers to add a MluI and AscI site to the 5' end and a HindIII site to the 3' end and then were subcloned into MluI and HindIII of the pAAV-hSyn-DIO-EGFP vector. The 1.8 kb promoter region of mouse Vglut2 was amplified from C57BL/6J whole brain genomic DNA with primers 5'-TCTTCC ACGCGT ACGCACTCCCCTGGTTGATTTAG-3' and 5'-TCTTCC GGCGCGCC TCTTGTAAGACTGGTGTCCAGCCT-3', digested with MluI and AscI and subcloned into pAAV-mCherry and pAAV-mCherry-2A-Cre. AAV9-hSyn-DIO-Ube3a and AAV2-hSyn-DIO-Cbln1-IRES-mCherry constructs were sent to the University of North Carolina Vector Core for viral particle production. AAV2/9-pVglut2-mCherry and AAV2/9-pVglut2-mCherry-2A-Cre constructs were sent to the Boston Children's Hospital Viral Core for viral particle production.

Brain slice patch clamp electrophysiology and *in vitro* optogenetics

Brains were rapidly removed and submerged in an ice-cold choline chloride replacement artificial cerebrospinal fluid (ACSF) containing (in mM): 126 choline chloride, 2.5 KCl, 1.2 NaH₂PO₄, 1.3 MgCl₂, 8 MgSO₄, 0.2 CaCl₂, 20 glucose, and 46 NaHCO₃, equilibrated with 95% O₂/5% CO₂. Coronal brain slices containing the nucleus accumbens (300 μ m thick) were made using a Leica VT1200S microtome (Leica Microsystems). The slices were placed in a holding chamber containing ACSF comprised of (mM): 124 NaCl, 3 KCl, 1 MgSO₄, 1.25 NaH₂PO₄, 2 CaCl₂, 25 Glucose, and 26 NaHCO₃, equilibrated with 95% O₂/5% CO₂. The slices were maintained at 33°C temperature for 30 minutes and then kept at room temperature until studied. To increase viability of neurons in the slices, 5 μ M glutathione, 500 μ M pyruvate, and 250 μ M kynurenic acid were added to the choline chloride replacement ACSF and ACSF in the holding chamber in all experiments. During recording, slices were superfused (2 ml/min) ACSF without glutathione, pyruvate and

kynurenic. Whole cell recordings were performed from neurons located in the nucleus accumbens (NAc) shell under visual control on an upright microscope with differential interference contrast and infrared illumination. Patch pipettes were pulled using a P-97 puller (Sutter Instruments) and filled with (mM): 130 K gluconate, 10 HEPES, 5 NaCl, 1 MgCl₂, 0.02 EGTA, 2 MgATP, 0.5 NaGTP and 10 mM sodium phosphocreatine at a pH of 7.3 and osmolality of 275 to 290 mOsm. 1 mM Alexa Fluor 568 hydrazide was dissolved in internal solution and was backfilled to the tip of the patch pipettes. Filled patch pipettes had resistances of 3–5 MΩ. Synaptic currents were recorded in voltage clamp mode by an Axon MultiClamp 700B amplifier (Molecular Devices). Data were filtered at 1 kHz, digitized at 10 kHz with DigiData 1440A interface (Molecular Devices) and acquired by Clampex 10.5. Medium spiny neurons (MSNs) were identified by their morphology and hyperpolarized resting membrane potential. Series resistance was monitored with a 5 mV hyperpolarizing step (5 ms). Resting membrane potential and action potentials (APs) were recorded in current clamp mode with APs induced by injecting 200 ms of positive currents ranging from 40 to 400 pA. An optical fiber (200 μm core diameter, 0.2 numerical apertures) was used to deliver optical stimulation. The fiber was placed 200 μm from the site of recording and coupled to a diode-pumped 473 nm laser (CrystaLaser Company) with stimulus intensity controlled from 1 to 30 mW. Light pulse duration (5ms) was controlled by a Master-8 stimulator and light pulse frequency (0.1 Hz) was determined and triggered by the Clampex 10.5. Light intensities of 0, 1, 5, and 30 mW were used for input/output experiments with six sweeps collected for each. 30 mW laser light was used for maximal stimulation and pharmacology experiments, 12 consecutive sweeps were averaged with Clampfit 10.5 to determine the light-evoked EPSC amplitude. 30 μM 6-cyano-7-nitroquinoxaline-2,3-dione (CNQX) was used in some studies to block and confirm AMPA receptor currents. Spontaneous EPSCs (sEPSCs) were recorded at a holding potential of –85 mV in the presence of GABA_A antagonist bicuculline (10 μM). sEPSCs were detected and analyzed using Mini Analysis Program (Synaptosoft, Decatur, GA). Amplitude and area thresholds were set to 5 pA and 20 fC, respectively. The peak amplitude and inter-event interval of sEPSCs from 60 s episodes were used to generate cumulative probability plots, and the statistical significance was determined by Kolmogorov-Smirnov test.

Statistics

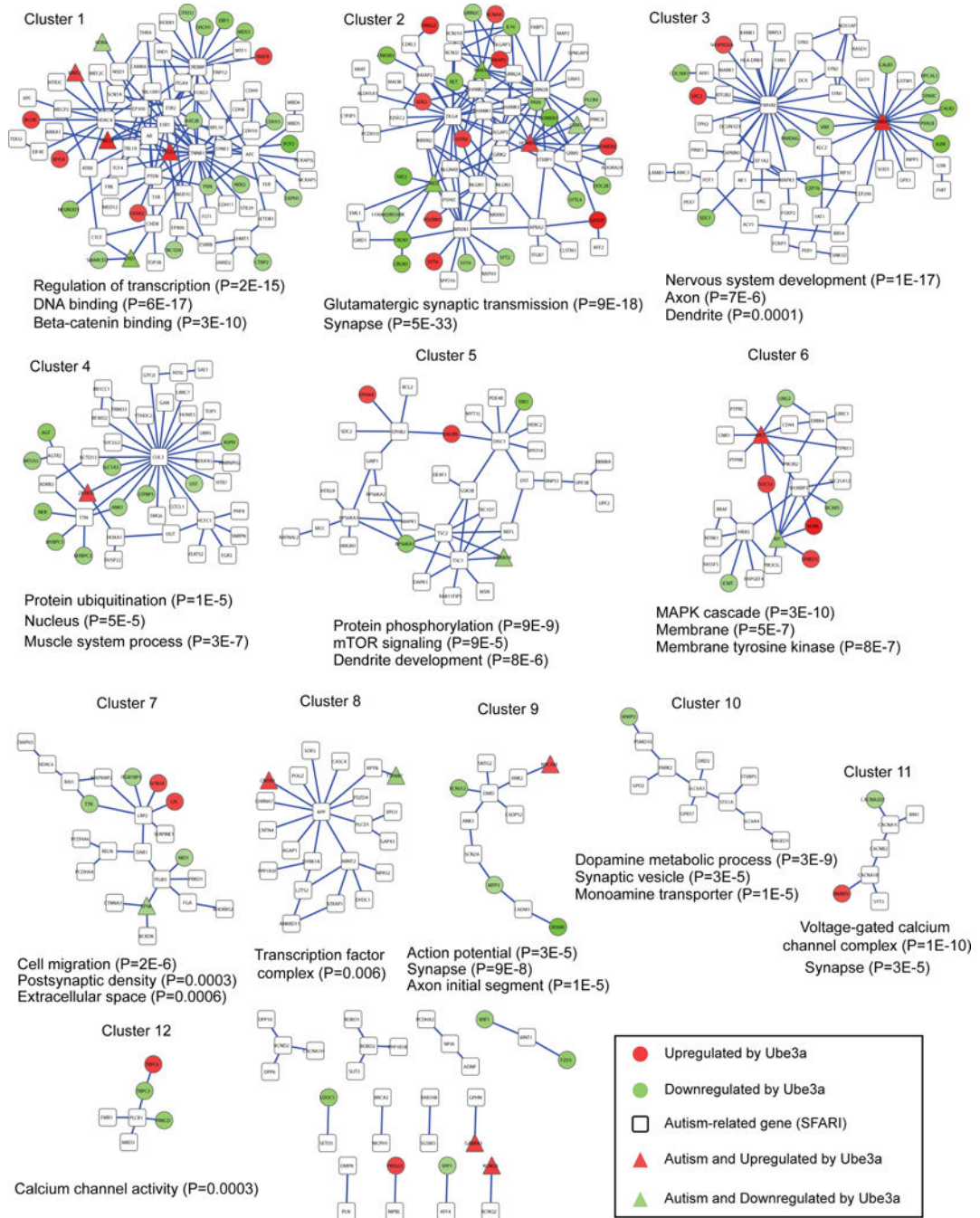
Sample sizes are shown in figures or legends and were chosen to meet or exceed sample sizes typically employed in similar mouse behavioral experiments. For three-chamber sociability experiments, “sniffing time” measures were entered into a two-way repeated measures ANOVA. F statistics and p values for “interaction effects” between *chamber side* (social versus opposite) or experimental group (various viruses, treatments or genotypes) and “main effects” are presented in Supplementary Table 5. When a significant *main effect* in either factor was detected (regardless of the presence of a statistical interaction), a Bonferroni post-hoc test was employed to obtain a p-value (adjusted for multiple comparisons) comparing the means of sniffing times for social and opposite conditions across groups^{22,62}. Thus, asterisks or “ns” (not significant) designations for all figures measuring three-chamber sociability represent the results of post-hoc comparisons. For experiments involving *LoxTBUbe3a* mice exclusively (Fig. 3a–i, Extended Data Fig. 8), the Holm-Sidak post-hoc test was employed. For all other experiments, an unpaired two-tailed

Student's T test was used to compare two groups, and a two-way ANOVA was employed to compare means across two or more dependent variables. A two way repeated measures ANOVA was utilized for rotarod testing (Extended Data Fig. 5k). Unless otherwise specified, data are presented as mean \pm standard error of the mean (SEM). $p < 0.05$ was considered statistically significant with *ns* indicating non-significant, * <0.05 , ** <0.01 , and *** <0.001 .

Data availability statement

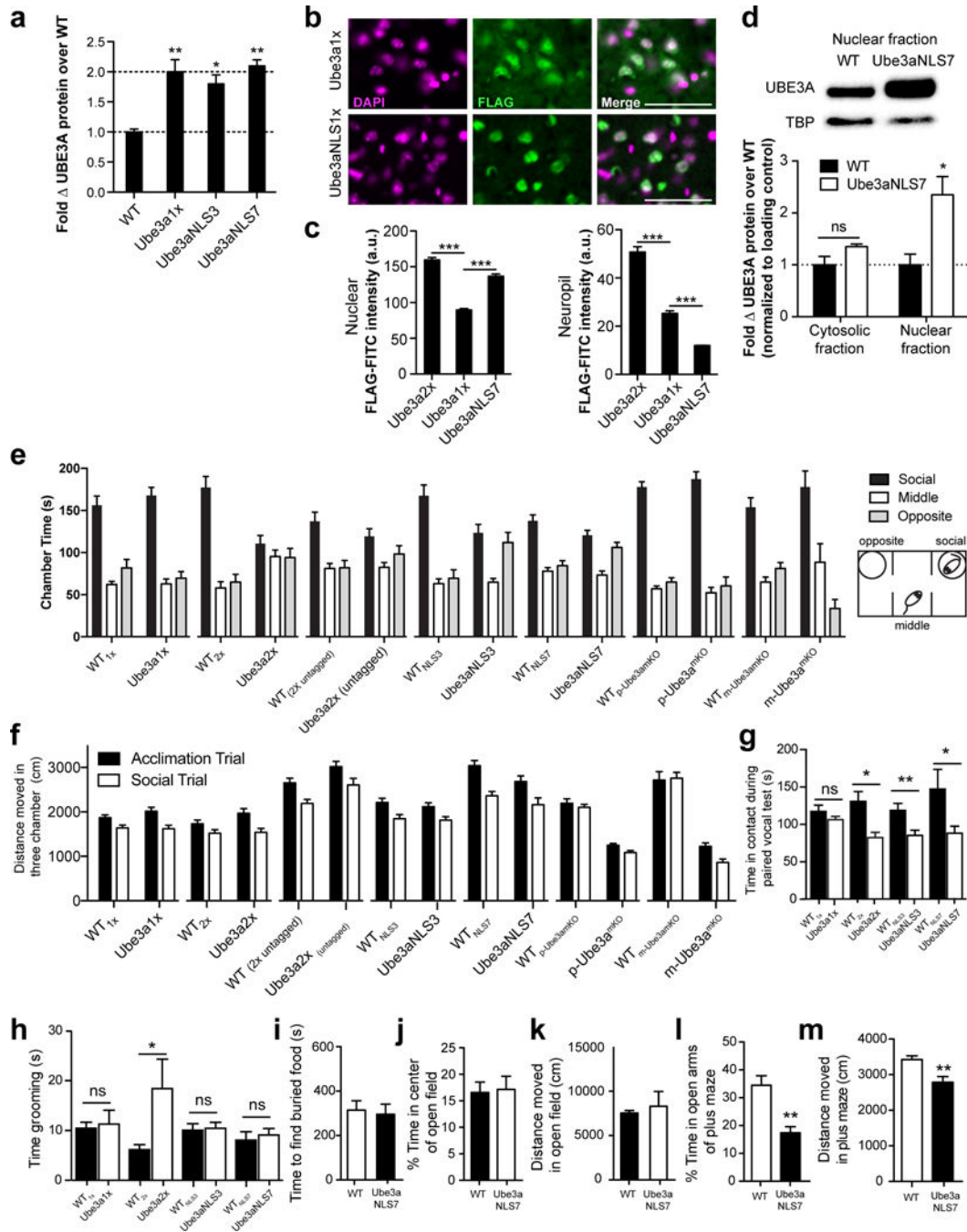
Source data are available for Figs 1, 2, 3, 4 and 5 and Extended Data Figs 2, 3, 4, 5, 6, 8, 9 and 10.

Extended Data



Extended Data Figure 1. Protein-protein interactions between genes regulated in Ube3a2x mice and autism-related genes

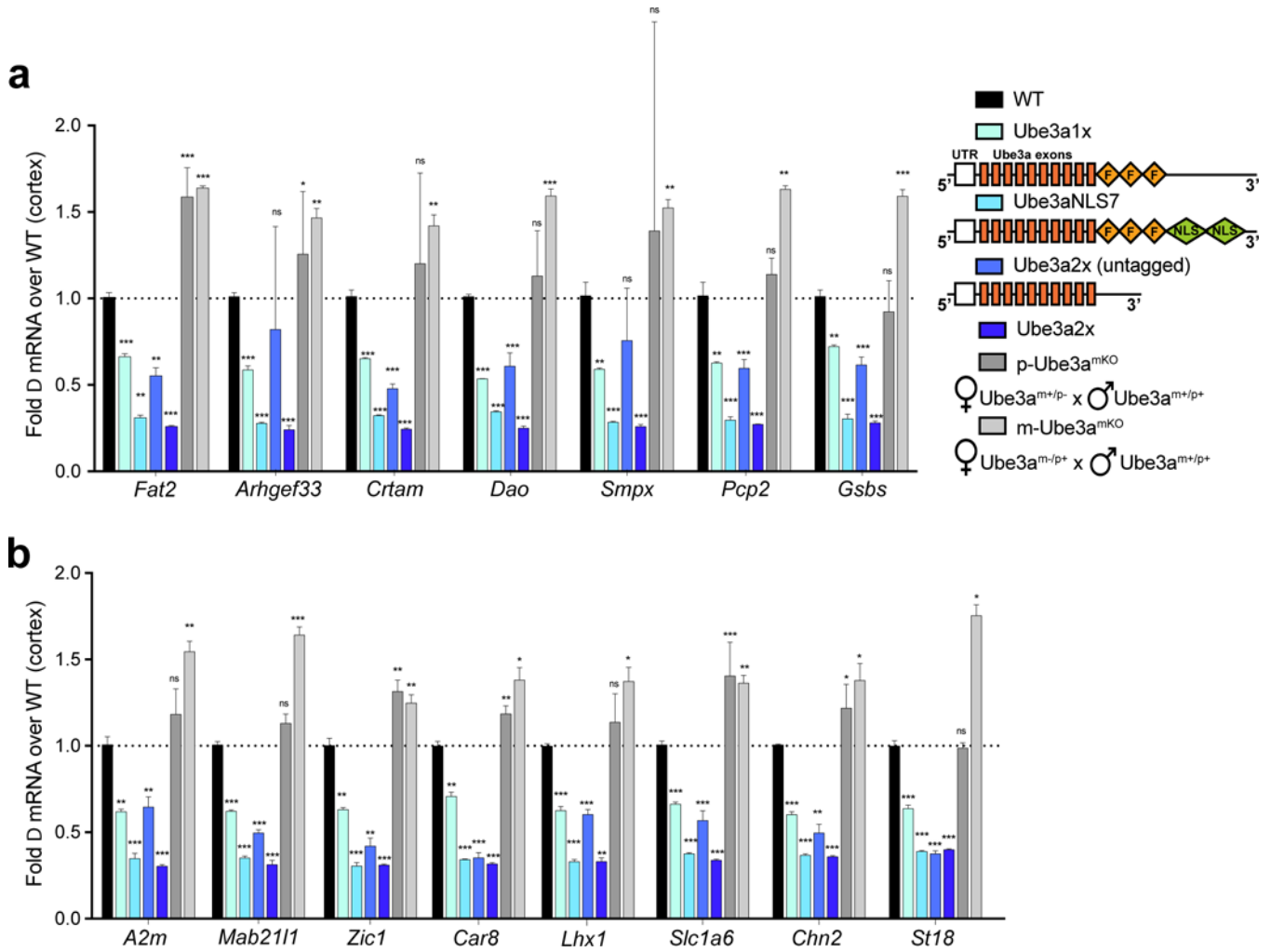
Edges between gene-labeled nodes represent documented protein-protein physical interactions. Clusters shown here are labeled with their major statistically significant gene ontology classification(s) together with *p* values representing significant enrichment. Within each cluster, all the genes (Ube3a-regulated and autism-related) were analyzed.



Extended Data Figure 2. Ube3aNLS mice and mice with increased untagged Ube3a levels display impaired sociability

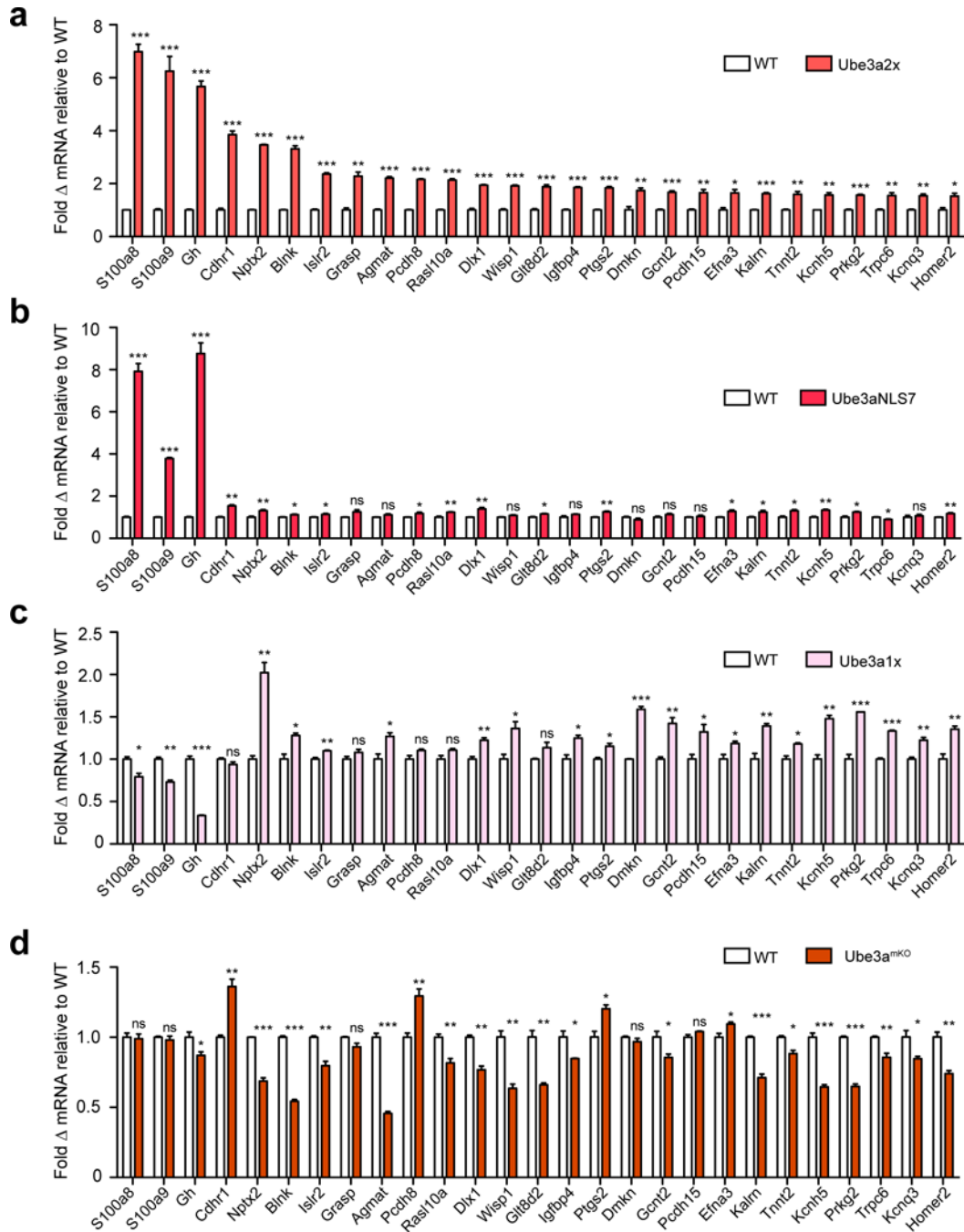
a, Total UBE3A protein levels by western blot in WT, Ube3a1x, Ube3aNLS3 and Ube3aNLS7 mice ($F_{[3,17]} = 12.30, p < 0.001, 5$ females/group). **b**, FLAG staining in Ube3a1x and Ube3aNLS mice, counterstained with DAPI (somatosensory cortex; 3 females/genotype; scale bar: 50 μ m). **c**, Quantified nuclear and neuropil FLAG immunofluorescence in arbitrary units (a.u.). **d**, UBE3A protein levels in cytosolic and nuclear fractions obtained from WT and Ube3aNLS7 mice (4 females/group), demonstrating a selective increase in

nuclear UBE3A protein levels (TBP: TATA-box binding protein, see Supplementary Figure 1). **e**, “Chamber times” (for Fig. 1d) during the social trial showing absolute times spent in “social”, “middle” and “opposite” chambers **f**, Distances moved during acclimation/social trials: WT/Ube3a1x (trial factor $F[1,56] = 18.09$, $p < 0.001$, genotype factor $F[1,56] = 0.73$, $p > 0.1$), WT/Ube3a2x (trial factor $F[1,52] = 12.2$, $p < 0.001$, genotype factor $F[1,52] = 2.046$, $p > 0.1$), WT/Ube3a2x untagged (trial factor $F[1,50] = 12.21$, $p < 0.01$, genotype factor $F[1,50] = 9.67$, $p < 0.01$), WT/Ube3aNLS3 (trial factor $F[1,56] = 14.41$, $p < 0.001$), genotype factor $F[1,56] = 0.53$, $p > 0.1$), WT/Ube3aNLS7 (trial factor $F[1,56] = 22.68$, $p < 0.001$, genotype factor $F[1,56] = 4.88$, $p < 0.05$), WT/p-Ube3a^{mKO} (trial factor $F[1,62] = 3.67$, $p > 0.05$, genotype factor $F[1,62] = 216.7$, $p < 0.0001$), WT/m-Ube3a^{mKO} (trial factor $F[1,48] = 1.75$, $p > 0.1$, genotype factor $F[1,48] = 197.9$, $p < 0.001$). **g**, Total time spent physically interacting during genotype-matched paired female interactions (for Fig. 1e). **h**, Time spent self-grooming by female mice during a 10 minute observation session across Ube3a1x (n=10 vs. n=14 WT), Ube3a2x (n=11 vs. n=12 WT), Ube3aNLS3 (14/group) and Ube3aNLS7 (n=14/group). **i**, Ube3aNLS7 (n=15) and WT (n=12) littermates take similar times to find a food item buried in fresh bedding. **j**, In an open field, Ube3aNLS7 and WT (n=5/group) littermates spend equal times in the center of an open field, and **k**, ambulate equal distances. **l**, In an elevated plus maze, Ube3aNLS7 (n=10) mice spend significantly less time in the open arms and **m**, ambulate slightly shorter distances overall than WT littermates (n=7). Mean \pm SEM plotted.



Extended Data Figure 3. Quantitative real-time PCR based validation of various genes downregulated in cortical samples from *Ube3a2x* mice

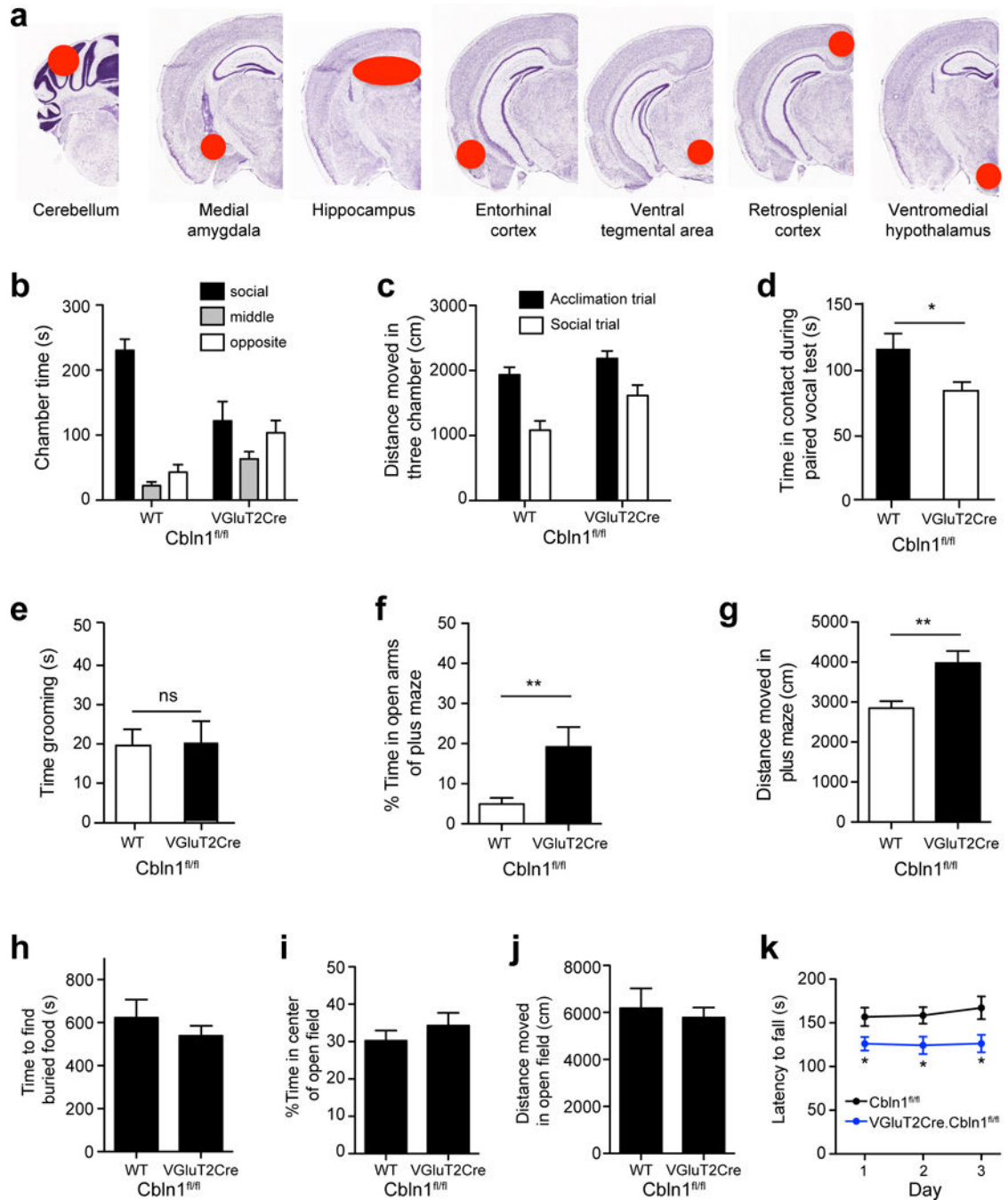
In separate cohorts of WT and *Ube3a* transgenic or *Ube3a*^{mKO} mice, we confirmed the downregulation of the following genes shown above in panels **a** and **b**: *Fat2* (FAT tumor suppressor homolog 2), *Arhgef33* (rho-guanine nucleotide exchange factor 33), *Crtam* (cytotoxic and T-cell regulatory molecule), *Dao* (D-amino acid oxidase), *Smpx* (small muscle protein, X-linked), *Pcp2* (Purkinje-cell protein 2), *Gsbs* (protein phosphatase 1, regulatory subunit 17), *A2m* (alpha-2 macroglobulin), *Mab2111* (mab-21-like 1), *Zic1* (zinc finger protein of the cerebellum 1), *Car8* (carbonic anhydrase 8), *Lhx1* (LIM homeobox protein 1), *Calb2* (Calbindin 2), *Slc1a6* (solute carrier family 1 [high affinity aspartate/ glutamate transporter]), *Chn2* (chimerin 2), *St18* (suppression of tumorigenicity 18). Sample sizes: *Ube3a1x*⁴, *Ube3aNLS*, *Ube3a2x*⁴, *m-Ube3a*^{mKO} 21 (n=3 pooled samples from two mice each), *Ube3a2x* (untagged) and *p-Ube3a*^{mKO} 5 (n=6–12/group, unpooled). Mean ± SEM plotted. Transgene constructs and/or breeding schemes are shown on the right.



Extended Data Figure 4. Quantitative real-time PCR based validation of various genes upregulated in cortical samples from *Ube3a2x* mice

a. In separate cohorts of WT and *Ube3a2x* mice, the upregulation of the following genes were confirmed by qRT-pCR: *s100a8* (s100 calcium binding protein A8), *s100a9* (s100 calcium binding protein A9), (*Gh* (growth hormone), *Cdhr1* (cadherin-related family member 1), *Nptx2* (neuronal pentraxin-2), *Blnk* (B-cell linker), *Islr2* (immunoglobulin superfamily containing leucine-rich repeat 2), *Grasp* (*Grp1* associated scaffold protein), *Agmat* (agmatine ureohydrolase), *Pcdh8* (protocadherin 8), *Rasi10a* (Ras-like, family 10, member A), *Dix1* (distal-less homebox 1), *Wisp1* (*Wnt1* associated signaling pathway

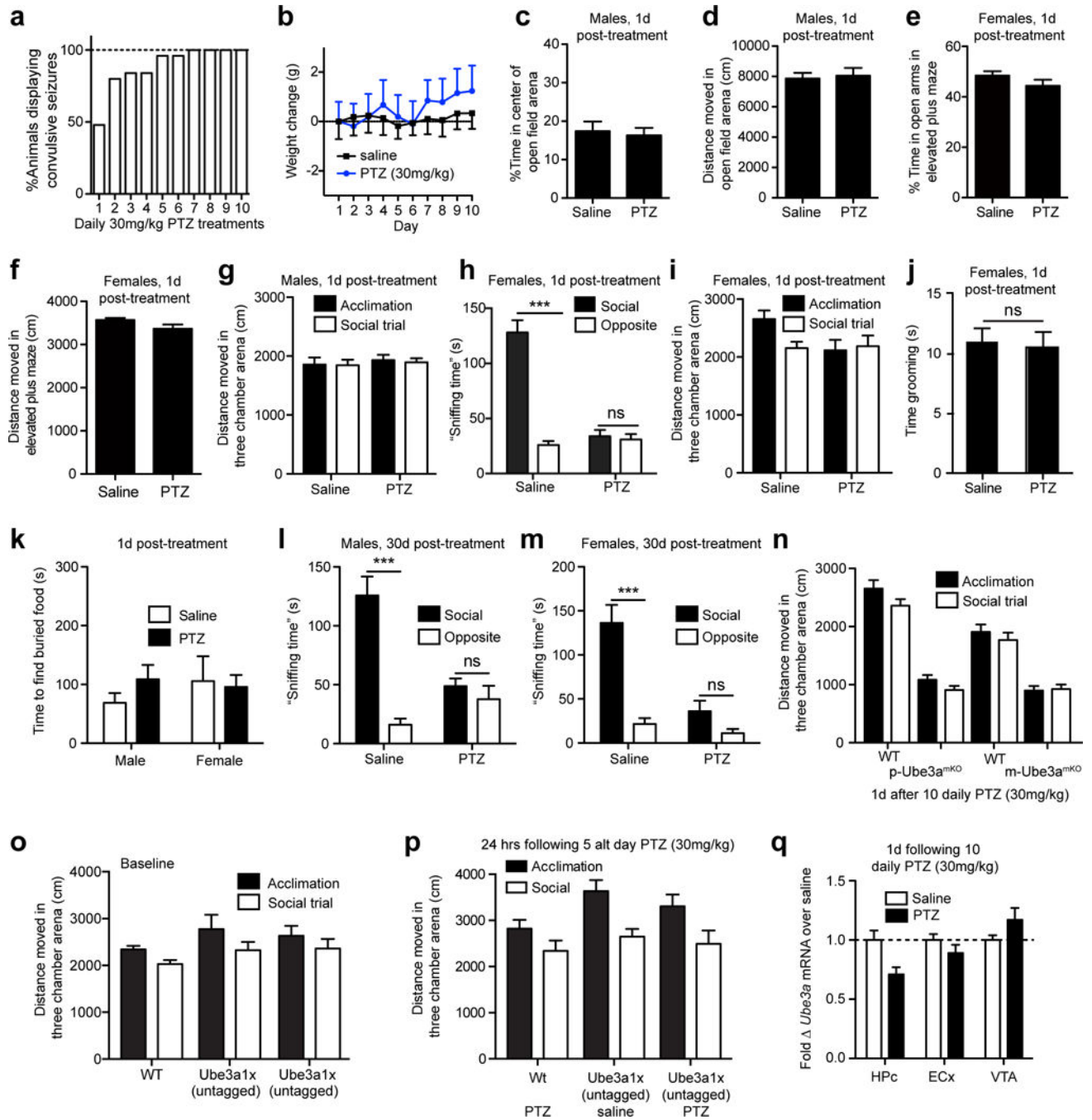
protein 1), *Glt8d2* (glycosyltransferase 8 containing domain 2), *Igfbp4* (insulin-like growth factor binding protein 4), *Ptgs2* (prostaglandin endoperoxide synthase 2), *Dmkn* (dermokine), *Gcnt2* (glucosaminyl [N-acetyl] transferase 2 I-branching enzyme), *Pcdh15* (protocadherin 15), *Efna3* (ephrin A3), *Kalrn* (kalirin, RhoGEF kinase), *Tnnt2* (troponin-2, cardiac), *Kcnh5* (potassium channel, voltage gated eag family related subfamily H, member 5), *Prkg2* (protein kinase, cGMP dependent 2), *Trpc6* (transient receptor potential cation channel, subfamily C, member 6), *Kcnq3* (potassium channel, voltage gated KQT-like subfamily Q, member 3), *Homer2* (homer homolog 2). **b**, Regulation of these genes in cortical samples from Ube3a^{NLS7}, **c**, Ube3a^{1x}, and **d**, Ube3a^{mKO} mice. n=3/genotype with each biological replicate representing a pooled sample of tissue from two genotype-matched mice. Mean ± SEM plotted.



Extended Data Figure 5. Characterization of VGluT2Cre.Cbln1^{fl/fl} mice

a, Representative coronal sections from the Allen Developing Mouse Brain Atlas⁶⁶ with shaded red regions depicting the approximate geometric center of punch biopsy samples used for quantitative real time PCR experiments (Image credit: Allen Institute). **b**, “Chamber times” (for Fig. 1g) during the social trial showing absolute time spent in “social”, “middle” and “opposite” chambers. **c**, Distances moved during acclimation/social trials (trial factor $F[1,32] = 27.21$, $p < 0.0001$, genotype factor $F[1,32] = 8.186$, $p < 0.01$). **d**, Total time spent physically interacting during genotype-matched paired female interactions (for Fig. 1h), and

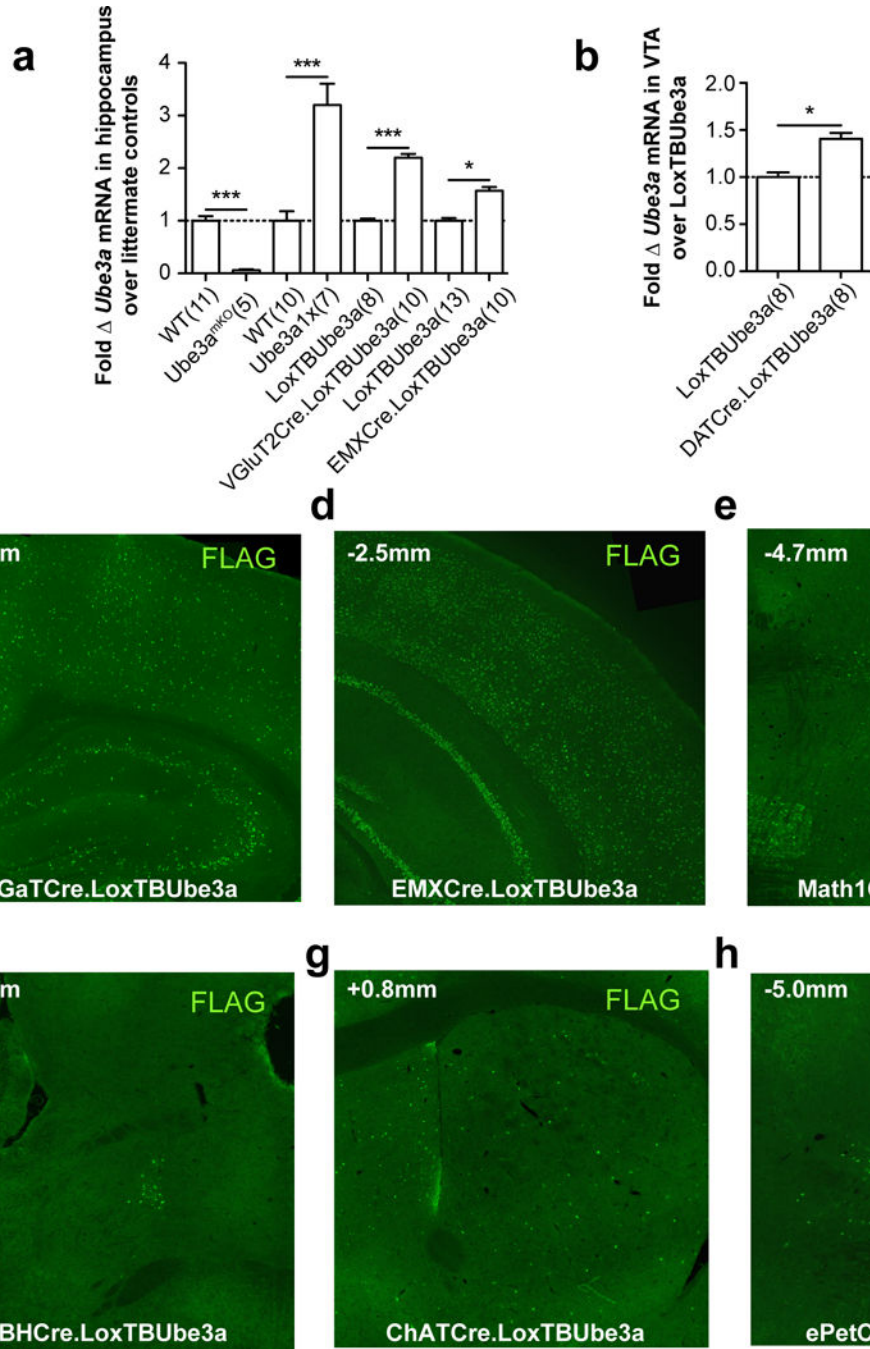
e, total time spent self-grooming during a 10 minute observation period (males only, n=8/group). **f**, In the elevated plus maze, VGluT2Cre.Cbln1^{fl/fl} (n=10) mice spent greater time in the open arms than Cbln1^{fl/fl} mice (n=8) and **g**, ambulated significantly greater distances. **h**, Performance of VGluT2Cre.Cbln1^{fl/fl} (n=16) and Cbln1^{fl/fl} (n=13) on buried food testing. Open field-testing of VGluT2Cre.Cbln1^{fl/fl} and Cbln1^{fl/fl} mice (n=10/group) with **i**, time in center, and **j**, distances moved. **k**, VGluT2Cre.Cbln1^{fl/fl} mice (n=16) display reduced latencies to fall off of an accelerating rotarod compared with Cbln1^{fl/fl} mice (n=13, genotype factor, $F[1, 81] = 18.10, p < 0.001$). Mean \pm SEM plotted.



Extended Data Figure 6. Recurrent seizures induced by pentylenetetrazole (PTZ) impair sociability

a, Ten daily 30 mg/kg PTZ injections applied to male WT mice resulted in a gradual daily increase in the percentage of animals that displayed a PTZ-induced generalized convulsion (n=25). **b**, Weight change for PTZ (n=10) or saline-treated mice (n=8), with test day factor $F[9,160] = 0.28$, $p > 0.1$, treatment factor $F[1,160] = 0.34$, $p > 0.1$. **c**, 24h following the last PTZ (n=16) or saline (n=14) injection, open field testing identified no significant differences in the time spent in the center of the field or **d**, total distance ambulated in the field (n=10/

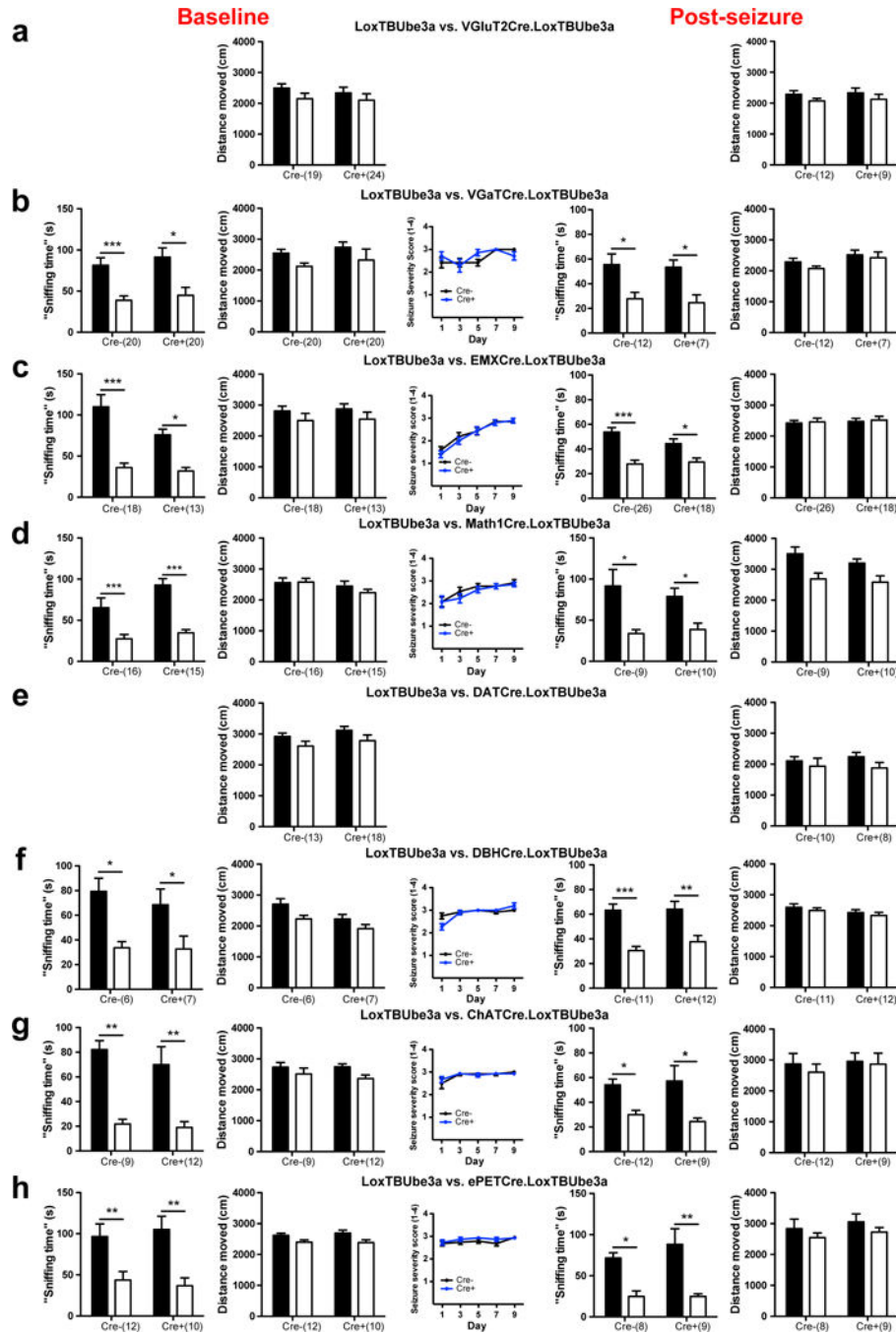
group). **e**, Similarly, on the elevated plus maze, 10 PTZ-induced seizures did not affect the time spent in the open arms or **f**, distance moved (n=10/group). **g**, Distances moved during acclimation/social trials for male mice (for Fig. 2b, treatment factor $F[1,32] = 0.38$, $p > 0.1$, trial factor $F[1,32] = 0.06$, $p > 0.1$). **h** Female WT FVB mice exposed to an identical 10 day PTZ (n=10) protocol demonstrated impaired sociability 24 hours following the last injection compared with mice that received saline alone (n=9), whereas **i**, distances moved during acclimation/social trials were not affected (treatment factor $F[1,34] = 2.47$, $p > 0.1$, trial factor $F[1,34] = 1.79$, $p > 0.1$). **j**, 10 PTZ-induced seizures do not impact self-grooming rates (n=10 females/group) or **k**, performance on the buried food test (males: saline 10, PTZ 7/group, females: saline 7, PTZ 9/group). **l**, 30 days following the last of 10 daily PTZ injections, male wild-type FVB mice continue to display impaired sociability (saline 10/group, PTZ 7/group), as do **m**, 10 daily PTZ-treated female mice (saline 6/group, PTZ 7/group). **n**, Distances moved during acclimation/social trials for Fig. 2f–g. WT/p-Ube3a^{mKO} (trial factor $F[1,62] = 5.06$, $p < 0.05$, genotype factor $F[1,62] = 209.2$, $p < 0.0001$) and WT/m-Ube3a^{mKO} (trial factor $F[1,54] = 0.20$, $p > 0.1$, genotype factor $F[1,54] = 56.06$, $p < 0.001$). **o**, Distances moved for Fig. 2h (trial factor $F[1,62] = 3.57$, $p > 0.05$, group factor $F[2,62] = 1.57$, $p > 0.05$). **p**, Distances moved for Fig. 2i (trial factor $F[1,62] = 13.29$, $p < 0.001$, group factor $F[2,62] = 2.43$, $p > 0.05$). **q**, *Ube3a* mRNA measured in punches from WT FVB males treated with ten daily injections of 30 mg/kg PTZ or saline (HPc, n=8/group, ECx and VTA: saline 10, PTZ 8). Mean \pm SEM plotted.



Extended Data Figure 7. Validation of “LoxTBube3a” mice

a, Quantitative real time PCR analysis of *Ube3a* mRNA from hippocampal samples (Extended Data Fig. 5a) demonstrating the up-regulation of *Ube3a* in VGluT2Cre.LoxTBube3a and EMXCre.LoxTBube3a mice. **b**, Similar analysis of *Ube3a* mRNA levels from punches of the ventral tegmental area of DATCre.LoxTBube3a mice (n=8/group). **c-h**, Spatial confirmation of FLAG staining in various “crosses” of LoxTBube3a mice confirming expression of *Ube3a* in inhibitory forebrain neurons (c), cortical and hippocampal neurons (d), scattered staining in midbrain and pontine nuclei (e),

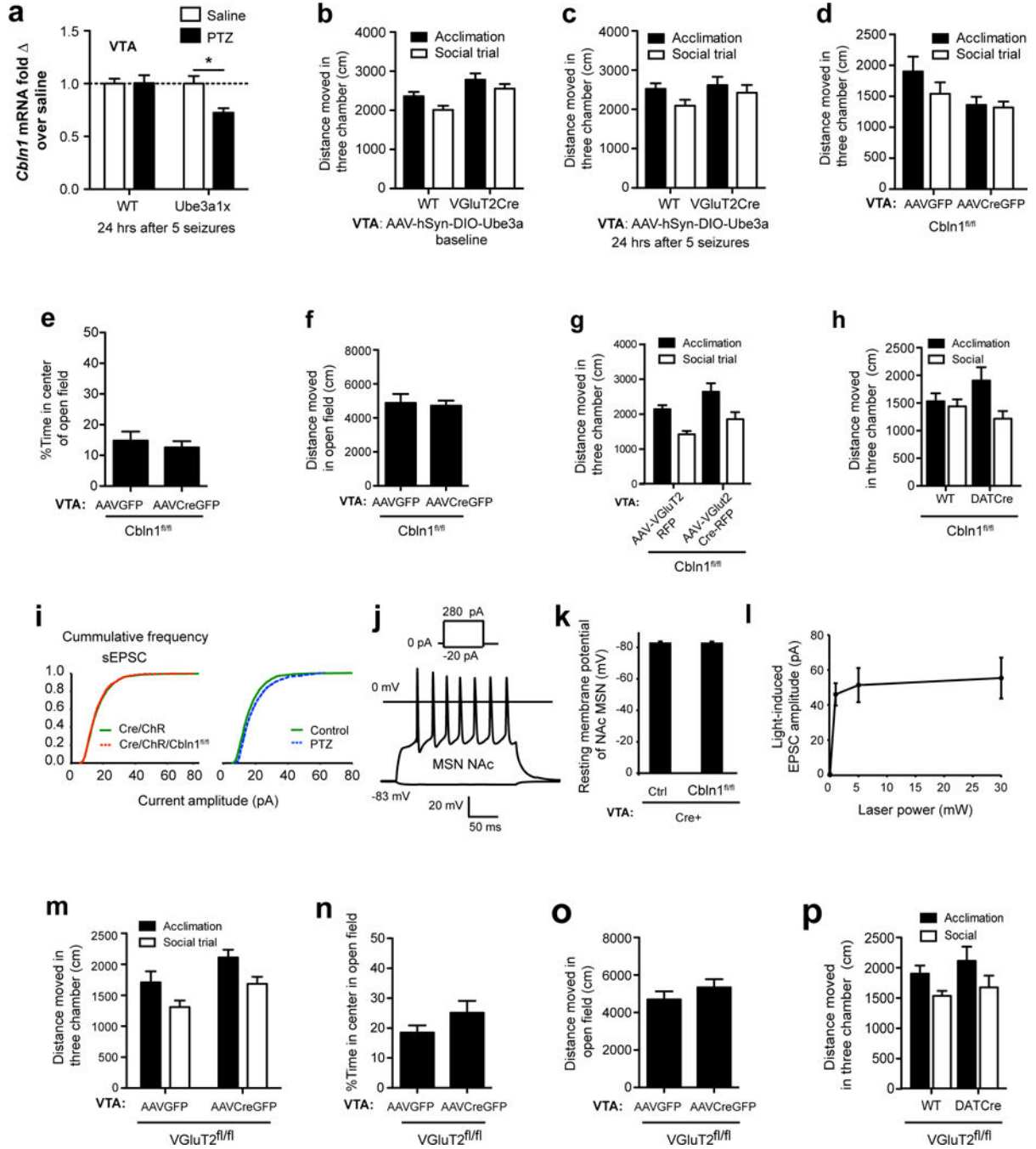
locus coeruleus (f), striatal cholinergic interneurons (g), and raphe regions (h), representative of n=2–3 mice/group. Mean ± SEM plotted.



Extended Data Figure 8. Targeted overexpression of *Ube3a* in VGLUT2 and DAT neurons increases the susceptibility to seizure-induced deficits in sociability

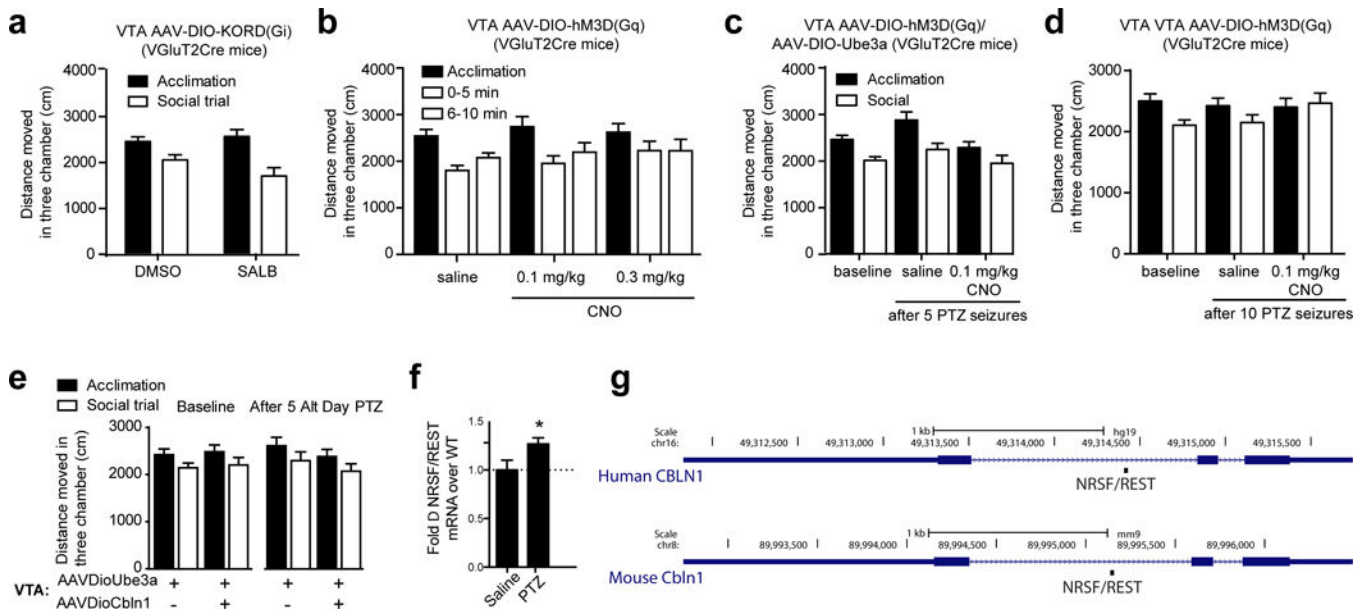
a–h, For each line of mice, we provide baseline “sniffing time” measures on sociability testing (far left), distances moved during this baseline test (second from left), seizure severity scores during five (alternate day) 30 mg/kg PTZ injections (middle), post-seizure “sniffing time” measures on three chamber testing (second from right) and associated

distances moved (far right). For sociability data, black and white bars represent “sniffing times” for social and opposite wire mesh cages respectively. For distance measures, black and white bars represent distances moved during acclimation and social trials respectively. For VGluT2Cre and DATCre lines, see Fig. 3c–e, g–i. Mean ± SEM plotted.



Extended Data Figure 9. Stereotaxic manipulations of *Ube3a*, *VGluT2* and *Cbln1* in VTA
a, qRT-PCR analysis of *Cbln1* mRNA in VTA punches of WT and Ube3a1x⁴ mice obtained 24h after the last of 5 alternate day PTZ injections. **b**, Distances moved during acclimation/

social trials for mice in Fig. 3k (genotype factor $F[1,28] = 14.45$, $p < 0.001$, trial factor $F[1,28] = 5.16$, $p < 0.05$). **c**, Distances moved for Fig. 3l (genotype factor $F[1,28] = 1.267$, $p > 0.1$, trial factor $F[1,28] = 2.72$, $p > 0.1$). **d**, Distances moved for Fig. 4a (virus factor $F[1,34] = 2.81$, $p > 0.1$, trial factor $F[1,34] = 2.02$, $p > 0.1$), or **e-f**, time spent in the center or the total distance moved in an open field for AAVCreGFP ($n=12$) or AAVGFP injected ($n=8$) *Cbln1*^{fl/fl} mice. **g**, Distances moved for Fig. 4b (virus factor $F[1,44] = 7.9$, $p < 0.01$, trial factor $F[1,44] = 20.49$, $p < 0.001$). **h**, Distances moved for Fig. 4c (genotype factor $F[1,26] = 0.22$, $p > 0.1$, trial factor $F[1,26] = 5.86$, $p < 0.05$). **i**, Cumulative frequency plots of sEPSC amplitudes for Fig. 4d,e. **j**, Representative response of a medium spiny neuron (MSN) to injected currents (-20 to $+280$ pA). **k**, Average resting membrane potentials in the nucleus accumbens (NAc) medial shell in control ($n=23$ neurons) and neurons from mice with VTA targeted AAV-CreGFP-mediated deletions of *Cbln1* ($n=22$ neurons, $p > 0.1$). **l**, Laser intensity needed to induce EPSC currents in medial shell NAc MSNs from ChR2-EYFP mice with AAV-CreGFP infused into VTA ($n=5$ neurons). **m**, Distances moved for Fig. 4i (trial factor $F[1,36] = 9.45$, $p < 0.01$, virus factor $F[1,36] = 8.49$, $p < 0.01$). **n,o** Time spent in the center and distances moved during the open field test following AAV-CreGFP mediated deletion of *VGlut2* in VTA ($n=8$). **p**, Distances moved for Fig. 4i (genotype factor $F[1,36] = 1.15$, $p > 0.1$, trial factor $F[1,36] = 6.18$, $p < 0.1$). Mean \pm SEM plotted.



Extended Data Figure 10. Chemogenetic manipulations of VTA VGlut2 neurons

a, Distances moved for Fig. 5a (trial factor $F[1,48] = 20.11$, $p < 0.001$, treatment factor $F[1,48] = 0.73$, $p > 0.5$). **b**, Distances moved for Fig. 5b (treatment factor $F[2,111] = 1.04$, $p > 0.5$, trial factor $F[2,111] = 9.55$, $p < 0.01$). **c**, Distances moved for Fig. 5c (trial factor $F[1,102] = 18.16$, $p < 0.0001$, group factor $F[2,102] = 5.7$, $p < 0.01$). **d**, Distances moved for Fig. 5d (trial factor $F[1,90] = 3.64$, $p > 0.05$, group factor $F[2,90] = 0.77$, $p > 0.05$). **e**, LEFT: Distances moved for Fig. 5e LEFT (trial factor $F[1,52] = 7.08$, $p < 0.05$, virus factor $F[1,52] = 0.022$, $p > 0.5$). RIGHT: Distances moved for Fig. 5e RIGHT (trial factor $F[1,76] = 8.48$, $p < 0.01$, virus factor $F[1,76] = 1.16$, $p > 0.05$). **f**, qRT-PCR analysis of *Rest* mRNA levels in

VTA 24h following 10 PTZ (n=8) or saline injections (n=10). **g**, Data presented from the Encode Project Consortium⁶⁷ showing locations of REST binding (also known as NRSF – neuronal restrictive silencing factor) within *Cbln1* intron of human (top) and mouse (bottom). Mean \pm SEM plotted.

Supplementary Material

Refer to Web version on PubMed Central for supplementary material.

Acknowledgments

We thank Oriana DiStefano, Greg Salimando, and Rebecca Broadhurst for colony work and the Harvard Medical School Neurobiology Imaging Facility (NINDS P30 Core Center Grant #NS07203) and Boston Children's Hospital IDDRC (1U54HD090255, P30HD18655). Supported by funding to V.K. (1R25NS070682 and an American Academy of Neurology Research Training Fellowship) and to M.P.A. from the NIH (1R01NS08916, 1R21MH100868, 1R21HD079249), Nancy Lurie Marks Family Foundation, Landreth Foundation, Simons Foundation, and Autism Speaks/National Alliance for Autism Research. R.A. supported by Klarman Family Foundation.

References

1. Chen JA, Penagarikano O, Belgard TG, Swarup V, Geschwind DH. The emerging picture of autism spectrum disorder: genetics and pathology. Annual review of pathology. 2015; 10:111–144. DOI: 10.1146/annurev-pathol-012414-040405
2. El Achkar CM, Spence SJ. Clinical characteristics of children and young adults with co-occurring autism spectrum disorder and epilepsy. *Epilepsy & behavior* : E&B. 2015
3. Glessner JT, et al. Autism genome-wide copy number variation reveals ubiquitous and neuronal genes. *Nature*. 2009; 459:569–573. DOI: 10.1038/nature07953 [PubMed: 19404257]
4. Smith SE, et al. Increased gene dosage of Ube3a results in autism traits and decreased glutamate synaptic transmission in mice. *Science translational medicine*. 2011; 3:103ra197.
5. Jiang YH, et al. Mutation of the Angelman ubiquitin ligase in mice causes increased cytoplasmic p53 and deficits of contextual learning and long-term potentiation. *Neuron*. 1998; 21:799–811. [PubMed: 9808466]
6. Kaphzan H, et al. Genetic reduction of the alpha1 subunit of Na/K-ATPase corrects multiple hippocampal phenotypes in Angelman syndrome. *Cell reports*. 2013; 4:405–412. DOI: 10.1016/j.celrep.2013.07.005 [PubMed: 23911285]
7. Matsuura T, et al. De novo truncating mutations in E6-AP ubiquitin-protein ligase gene (UBE3A) in Angelman syndrome. *Nature genetics*. 1997; 15:74–77. DOI: 10.1038/ng0197-74 [PubMed: 8988172]
8. Wallace ML, Burette AC, Weinberg RJ, Philpot BD. Maternal loss of Ube3a produces an excitatory/inhibitory imbalance through neuron type-specific synaptic defects. *Neuron*. 2012; 74:793–800. DOI: 10.1016/j.neuron.2012.03.036 [PubMed: 22681684]
9. Scheffner M, Huibregtse JM, Vierstra RD, Howley PM. The HPV-16 E6 and E6-AP complex functions as a ubiquitin-protein ligase in the ubiquitination of p53. *Cell*. 1993; 75:495–505. [PubMed: 8221889]
10. Nawaz Z, et al. The Angelman syndrome-associated protein, E6-AP, is a coactivator for the nuclear hormone receptor superfamily. *Molecular and cellular biology*. 1999; 19:1182–1189. [PubMed: 9891052]
11. Scoles HA, Urraca N, Chadwick SW, Reiter LT, Lasalle JM. Increased copy number for methylated maternal 15q duplications leads to changes in gene and protein expression in human cortical samples. *Molecular autism*. 2011; 2:19. [PubMed: 22152151]
12. Basu SN, Kollu R, Banerjee-Basu S. AutDB: a gene reference resource for autism research. *Nucleic acids research*. 2009; 37:D832–836. DOI: 10.1093/nar/gkn835 [PubMed: 19015121]

13. Matsuda K, Yuzaki M. Cbln family proteins promote synapse formation by regulating distinct neurexin signaling pathways in various brain regions. *The European journal of neuroscience*. 2011; 33:1447–1461. DOI: 10.1111/j.1460-9568.2011.07638.x [PubMed: 21410790]
14. Wei P, et al. The Cbln family of proteins interact with multiple signaling pathways. *Journal of neurochemistry*. 2012; 121:717–729. DOI: 10.1111/j.1471-4159.2012.07648.x [PubMed: 22220752]
15. Elegheert J, et al. Structural basis for integration of GluD receptors within synaptic organizer complexes. *Science*. 2016; 353:295–299. DOI: 10.1126/science.aae0104 [PubMed: 27418511]
16. Matsuda K, et al. Cbln1 is a ligand for an orphan glutamate receptor delta2, a bidirectional synapse organizer. *Science*. 2010; 328:363–368. DOI: 10.1126/science.1185152 [PubMed: 20395510]
17. Uemura T, et al. Trans-synaptic interaction of GluRdelta2 and Neurexin through Cbln1 mediates synapse formation in the cerebellum. *Cell*. 2010; 141:1068–1079. DOI: 10.1016/j.cell.2010.04.035 [PubMed: 20537373]
18. Ryu K, Yokoyama M, Yamashita M, Hirano T. Induction of excitatory and inhibitory presynaptic differentiation by GluD1. *Biochemical and biophysical research communications*. 2012; 417:157–161. DOI: 10.1016/j.bbrc.2011.11.075 [PubMed: 22138648]
19. Hirai H, et al. Cbln1 is essential for synaptic integrity and plasticity in the cerebellum. *Nature neuroscience*. 2005; 8:1534–1541. DOI: 10.1038/nn1576 [PubMed: 16234806]
20. Bao D, et al. Cbln1 is essential for interaction-dependent secretion of Cbln3. *Molecular and cellular biology*. 2006; 26:9327–9337. DOI: 10.1128/MCB.01161-06 [PubMed: 17030622]
21. Grier MD, Carson RP, Lagrange AH. Of mothers and myelin: Aberrant myelination phenotypes in mouse model of Angelman syndrome are dependent on maternal and dietary influences. *Behavioural brain research*. 2015; 291:260–267. DOI: 10.1016/j.bbr.2015.05.045 [PubMed: 26028516]
22. Yang M, Silverman JL, Crawley JN. Automated three-chambered social approach task for mice. *Current protocols in neuroscience / editorial board, Jacqueline N. Crawley ... [et al.]*. 2011:26. Chapter 8. Unit 8.
23. Yadav R, et al. Deletion of glutamate delta-1 receptor in mouse leads to aberrant emotional and social behaviors. *PloS one*. 2012; 7:e32969. [PubMed: 22412961]
24. Iijima T, Emi K, Yuzaki M. Activity-dependent repression of Cbln1 expression: mechanism for developmental and homeostatic regulation of synapses in the cerebellum. *The Journal of neuroscience : the official journal of the Society for Neuroscience*. 2009; 29:5425–5434. DOI: 10.1523/JNEUROSCI.4473-08.2009 [PubMed: 19403810]
25. Takechi K, Suemaru K, Kiyoi T, Tanaka A, Araki H. The alpha4beta2 nicotinic acetylcholine receptor modulates autism-like behavioral and motor abnormalities in pentylentetrazol-kindled mice. *Eur J Pharmacol*. 2016; 775:57–66. DOI: 10.1016/j.ejphar.2016.02.021 [PubMed: 26868186]
26. Taylor SR, et al. GABAergic and glutamatergic efferents of the mouse ventral tegmental area. *The Journal of comparative neurology*. 2014; 522:3308–3334. DOI: 10.1002/cne.23603 [PubMed: 24715505]
27. Zhang S, et al. Dopaminergic and glutamatergic microdomains in a subset of rodent mesoaccumbens axons. *Nature neuroscience*. 2015; 18:386–392. DOI: 10.1038/nn.3945 [PubMed: 25664911]
28. Gunaydin LA, et al. Natural neural projection dynamics underlying social behavior. *Cell*. 2014; 157:1535–1551. DOI: 10.1016/j.cell.2014.05.017 [PubMed: 24949967]
29. Yamaguchi T, Qi J, Wang HL, Zhang S, Morales M. Glutamatergic and dopaminergic neurons in the mouse ventral tegmental area. *The European journal of neuroscience*. 2015; 41:760–772. DOI: 10.1111/ejn.12818 [PubMed: 25572002]
30. Greer PL, et al. The Angelman Syndrome protein Ube3A regulates synapse development by ubiquitinating arc. *Cell*. 2010; 140:704–716. DOI: 10.1016/j.cell.2010.01.026 [PubMed: 20211139]
31. Khan OY, et al. Multifunction steroid receptor coactivator, E6-associated protein, is involved in development of the prostate gland. *Molecular endocrinology*. 2006; 20:544–559. DOI: 10.1210/me.2005-0110 [PubMed: 16254014]

32. Kuhnle S, Mothes B, Matentzoglou K, Scheffner M. Role of the ubiquitin ligase E6AP/UBE3A in controlling levels of the synaptic protein Arc. *Proceedings of the National Academy of Sciences of the United States of America*. 2013; 110:8888–8893. DOI: 10.1073/pnas.1302792110 [PubMed: 23671107]
33. Kim S, Chahrour M, Ben-Shachar S, Lim J. Ube3a/E6AP is involved in a subset of MeCP2 functions. *Biochemical and biophysical research communications*. 2013; 437:67–73. DOI: 10.1016/j.bbrc.2013.06.036 [PubMed: 23791832]
34. Lyst MJ, et al. Rett syndrome mutations abolish the interaction of MeCP2 with the NCoR/SMRT co-repressor. *Nature neuroscience*. 2013; 16:898–902. DOI: 10.1038/nn.3434 [PubMed: 23770565]
35. McClelland S, et al. The transcription factor NRSF contributes to epileptogenesis by selective repression of a subset of target genes. *Elife*. 2014; 3:e01267. [PubMed: 25117540]
36. Liu M, et al. Neuronal conditional knockout of NRSF decreases vulnerability to seizures induced by pentylenetetrazol in mice. *Acta Biochim Biophys Sin (Shanghai)*. 2012; 44:476–482. DOI: 10.1093/abbs/gms023 [PubMed: 22472570]
37. Kent WJ, et al. The human genome browser at UCSC. *Genome Res*. 2002; 12:996–1006. Article published online before print in May 2002. DOI: 10.1101/gr.229102 [PubMed: 12045153]
38. Yi JJ, et al. An Autism-Linked Mutation Disables Phosphorylation Control of UBE3A. *Cell*. 2015; 162:795–807. DOI: 10.1016/j.cell.2015.06.045 [PubMed: 26255772]
39. Ronchi VP, Klein JM, Edwards DJ, Haas AL. The active form of E6-associated protein (E6AP)/UBE3A ubiquitin ligase is an oligomer. *The Journal of biological chemistry*. 2014; 289:1033–1048. DOI: 10.1074/jbc.M113.517805 [PubMed: 24273172]
40. Gossan NC, et al. The E3 ubiquitin ligase UBE3A is an integral component of the molecular circadian clock through regulating the BMAL1 transcription factor. *Nucleic acids research*. 2014; 42:5765–5775. DOI: 10.1093/nar/gku225 [PubMed: 24728990]
41. Berrios J, et al. Loss of UBE3A from TH-expressing neurons suppresses GABA co-release and enhances VTA-NAc optical self-stimulation. *Nature communications*. 2016; 7:10702.
42. Riday TT, et al. Pathway-specific dopaminergic deficits in a mouse model of Angelman syndrome. *The Journal of clinical investigation*. 2012; 122:4544–4554. DOI: 10.1172/JCI61888 [PubMed: 23143301]
43. Zhou YD, et al. Arrested maturation of excitatory synapses in autosomal dominant lateral temporal lobe epilepsy. *Nature medicine*. 2009; 15:1208–1214. DOI: 10.1038/nm.2019
44. Anderson MP, et al. Thalamic Cav3.1 T-type Ca²⁺ channel plays a crucial role in stabilizing sleep. *Proceedings of the National Academy of Sciences of the United States of America*. 2005; 102:1743–1748. DOI: 10.1073/pnas.0409644102 [PubMed: 15677322]
45. Srinivas S, et al. Cre reporter strains produced by targeted insertion of EYFP and ECFP into the ROSA26 locus. *BMC developmental biology*. 2001; 1:4. [PubMed: 11299042]
46. Salvat C, Wang G, Dastur A, Lyon N, Huijbregtse JM. The -4 phenylalanine is required for substrate ubiquitination catalyzed by HECT ubiquitin ligases. *The Journal of biological chemistry*. 2004; 279:18935–18943. DOI: 10.1074/jbc.M312201200 [PubMed: 14966115]
47. Vong L, et al. Leptin action on GABAergic neurons prevents obesity and reduces inhibitory tone to POMC neurons. *Neuron*. 2011; 71:142–154. DOI: 10.1016/j.neuron.2011.05.028 [PubMed: 21745644]
48. Tong Q, et al. Synaptic glutamate release by ventromedial hypothalamic neurons is part of the neurocircuitry that prevents hypoglycemia. *Cell metabolism*. 2007; 5:383–393. DOI: 10.1016/j.cmet.2007.04.001 [PubMed: 17488640]
49. Gorski JA, et al. Cortical excitatory neurons and glia, but not GABAergic neurons, are produced in the Emx1-expressing lineage. *The Journal of neuroscience : the official journal of the Society for Neuroscience*. 2002; 22:6309–6314. doi:20026564. [PubMed: 12151506]
50. Rose MF, Ahmad KA, Thaller C, Zoghbi HY. Excitatory neurons of the proprioceptive, interoceptive, and arousal hindbrain networks share a developmental requirement for Math1. *Proceedings of the National Academy of Sciences of the United States of America*. 2009; 106:22462–22467. DOI: 10.1073/pnas.0911579106 [PubMed: 20080794]

51. Zhuang X, Masson J, Gingrich JA, Rayport S, Hen R. Targeted gene expression in dopamine and serotonin neurons of the mouse brain. *Journal of neuroscience methods*. 2005; 143:27–32. DOI: 10.1016/j.jneumeth.2004.09.020 [PubMed: 15763133]
52. Kobayashi K, et al. Survival of developing motor neurons mediated by Rho GTPase signaling pathway through Rho-kinase. *The Journal of neuroscience : the official journal of the Society for Neuroscience*. 2004; 24:3480–3488. DOI: 10.1523/JNEUROSCI.0295-04.2004 [PubMed: 15071095]
53. Rossi J, et al. Melanocortin-4 receptors expressed by cholinergic neurons regulate energy balance and glucose homeostasis. *Cell metabolism*. 2011; 13:195–204. DOI: 10.1016/j.cmet.2011.01.010 [PubMed: 21284986]
54. Scott MM, Williams KW, Rossi J, Lee CE, Elmquist JK. Leptin receptor expression in hindbrain Glp-1 neurons regulates food intake and energy balance in mice. *The Journal of clinical investigation*. 2011; 121:2413–2421. DOI: 10.1172/JCI43703 [PubMed: 21606595]
55. Madisen L, et al. A toolbox of Cre-dependent optogenetic transgenic mice for light-induced activation and silencing. *Nature neuroscience*. 2012; 15:793–802. DOI: 10.1038/nn.3078 [PubMed: 22446880]
56. Rozen S, Skaletsky H. Primer3 on the WWW for general users and for biologist programmers. *Methods in molecular biology*. 2000; 132:365–386. [PubMed: 10547847]
57. Ye J, et al. Primer-BLAST: a tool to design target-specific primers for polymerase chain reaction. *BMC bioinformatics*. 2012; 13:134. [PubMed: 22708584]
58. Schmittgen TD, Livak KJ. Analyzing real-time PCR data by the comparative C(T) method. *Nature protocols*. 2008; 3:1101–1108. [PubMed: 18546601]
59. Ashburner M, et al. Gene ontology: tool for the unification of biology. The Gene Ontology Consortium. *Nature genetics*. 2000; 25:25–29. DOI: 10.1038/75556 [PubMed: 10802651]
60. Gentleman RC, et al. Bioconductor: open software development for computational biology and bioinformatics. *Genome biology*. 2004; 5:R80. [PubMed: 15461798]
61. Smoot ME, Ono K, Ruscheinski J, Wang PL, Ideker T. Cytoscape 2.8: new features for data integration and network visualization. *Bioinformatics*. 2011; 27:431–432. DOI: 10.1093/bioinformatics/btq675 [PubMed: 21149340]
62. Silverman JL, et al. GABAB Receptor Agonist R-Baclofen Reverses Social Deficits and Reduces Repetitive Behavior in Two Mouse Models of Autism. *Neuropsychopharmacology : official publication of the American College of Neuropsychopharmacology*. 2015; 40:2228–2239. DOI: 10.1038/npp.2015.66 [PubMed: 25754761]
63. Allensworth M, Saha A, Reiter LT, Heck DH. Normal social seeking behavior, hypoactivity and reduced exploratory range in a mouse model of Angelman syndrome. *BMC genetics*. 2011; 12:7. [PubMed: 21235769]
64. Yang M, Crawley JN. Simple behavioral assessment of mouse olfaction. *Current protocols in neuroscience / editorial board, Jacqueline N. Crawley ... [et al.]*. 2009:24. Chapter 8. Unit 8.
65. Ferraro TN, et al. Mapping loci for pentylentetrazol-induced seizure susceptibility in mice. *The Journal of neuroscience : the official journal of the Society for Neuroscience*. 1999; 19:6733–6739. [PubMed: 10436030]
66. Lein ES, et al. Genome-wide atlas of gene expression in the adult mouse brain. *Nature*. 2007; 445:168–176. DOI: 10.1038/nature05453 [PubMed: 17151600]
67. Consortium EP. An integrated encyclopedia of DNA elements in the human genome. *Nature*. 2012; 489:57–74. DOI: 10.1038/nature11247 [PubMed: 22955616]

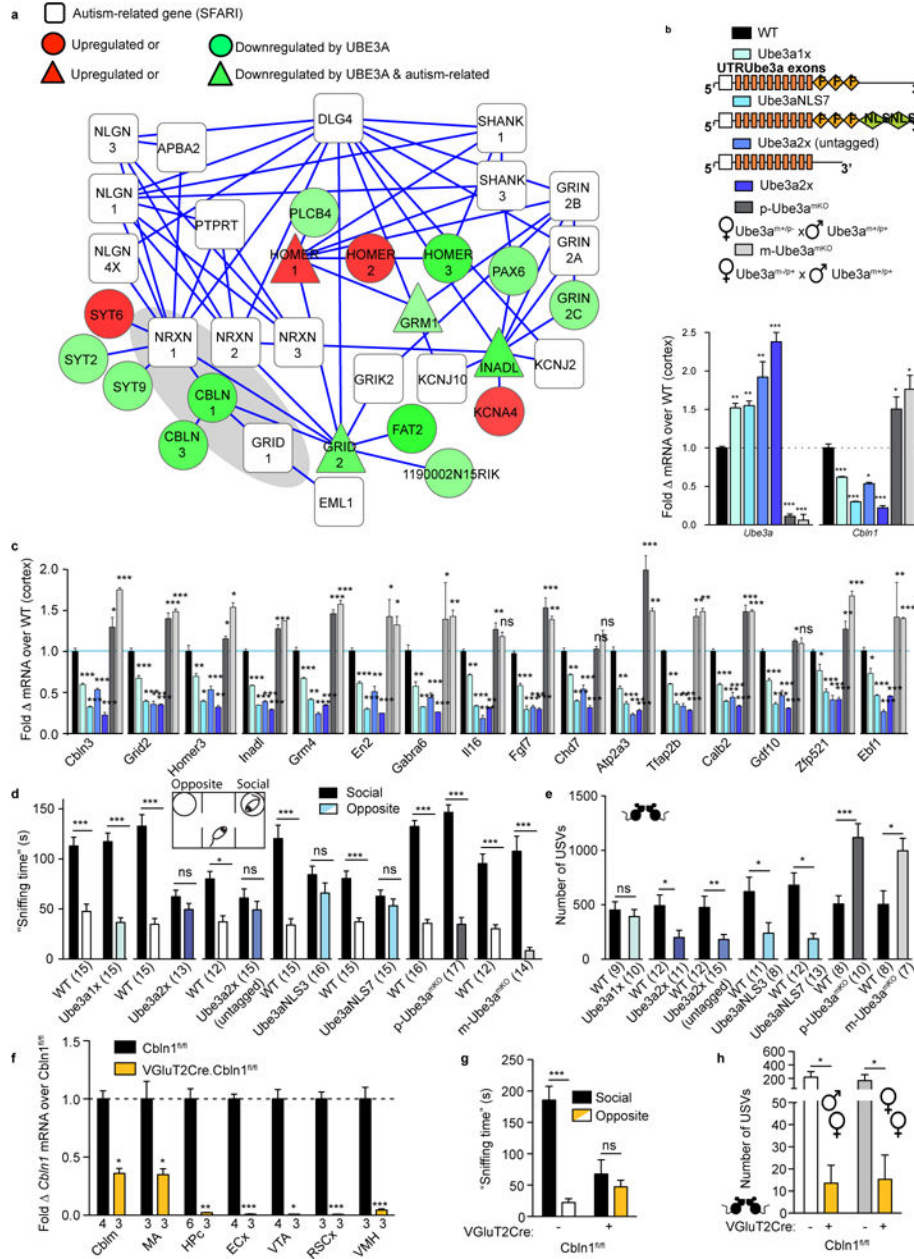


Figure 1. Nuclear-targeted increases of UBE3A repress ASD network gene *Cbln1* that is required in *VGluT2* neurons for sociability

a, Protein interaction sub-cluster enriched for glutamatergic synapse proteins encoded by autism-linked¹³ and *Ube3a* up- and down-regulated genes. **b**, q-RT-PCR validates *Cbln1* in *Ube3a1x*⁴, *Ube3aNLS*, *Ube3a2x*⁴, *m-Ube3a*^{mKO} 21 (n=3 pooled samples of two mice each), *Ube3a2x* (untagged) and *p-Ube3a*^{mKO} 5 (n=6–12/group). Transgene constructs or breeding strategy schematic shown (F: FLAG-tags, NLS: nuclear localization signal). **c**, q-RT-PCR validates *Cbln3* (Cerebellin-3), *Grid-2* (glutamate receptor ionotropic delta subunit-2), *Homer-3*, *Inadl* (InaD-like), *Grm4* (Glutamate receptor metabotropic 4), *En2* (engrailed-2), *Gabra6* (GABA-A subunit alpha 6), *Il16* (interleukin-16), *Fgf7* (fibroblast growth factor 7), *Chd7* (chomodomain helicase DNA binding protein 7), *Atp2a3* (ATPase Calcium

transporting ubiquitous), *Tfap2b* (transcription factor AP-2 beta), *Calb2* (Calbindin 2), *Gdf10* (growth differentiation factor 10), *Zfp521* (Zinc finger protein 521), *Ebf1* (early B-cell factor 1). **d**, Sociability of female mutant/transgenic and WT littermate mice. **e**, USVs during genotype-matched pairings. **f**, qRT-PCR for *Cbln1* (Cblm: cerebellum, MA: medial amygdala, HPc: hippocampus, ECx: entorhinal cortex, VTA: ventral tegmental area, RSCx: retrosplenial cortex, VMH: ventromedial hypothalamus); **g**, sociability (Cre- n=8, Cre+ n=10); and **h**, USVs in male-female (Cre- n=14, Cre+ n=8) and genotype-matched female-female pairs (Cre- n=11, Cre+ n=16). Mean \pm SEM plotted. For three-chamber experiments, “sniffing time” analyzed by two-way repeated-measures ANOVA. F statistics and p values for “interaction effects” between *chamber side* (social versus opposite) or experimental group (viruses, treatments or genotypes) and “main effects” in Supplementary Table 5. For significant *interaction* and/or *main effects*, a Bonferroni post-hoc test p-value is reported (adjusted for multiple comparisons, corresponding to * or ns [not significant] designations).

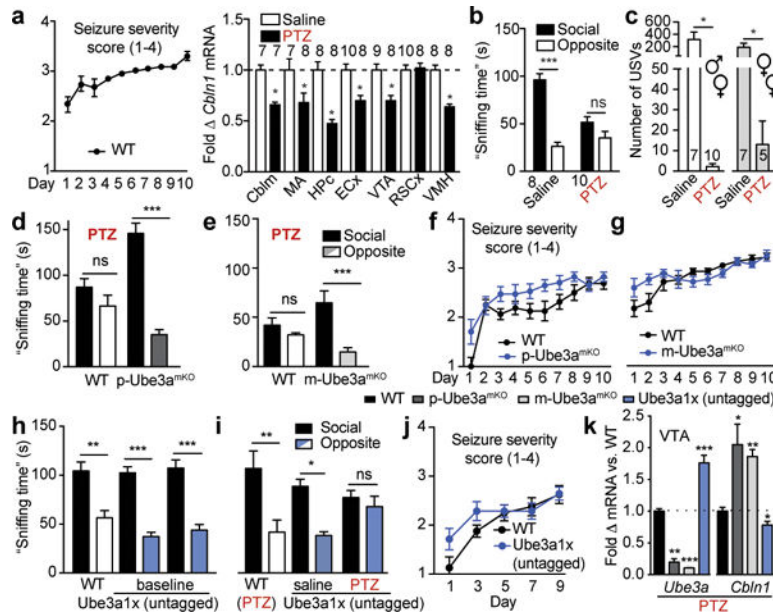


Figure 2. Seizures synergize with increased UBE3A to repress sociability and *Cbln1*
a, LEFT: Seizure severity during 10 daily 30mg/kg PTZ doses in WT (n=25 males) and RIGHT, qRT-PCR for *Cbln1* 24h after last PTZ injection. **b**, Sociability (males), and **c**, USVs in male-female and treatment-matched female pairs. Seizure severity with 10 daily PTZ (30 mg/kg) and sociability 24h after last PTZ dose in **d,f**, WT (n=16) vs. p-Ube3a^{mKO} (n=17) and **e,g**, WT (n=18) and m-Ube3a^{mKO} (n=11). **h**, Baseline sociability, **i**, post-seizure sociability and **j**, seizure severity scores during the five day “subthreshold” PTZ paradigm in WT mice (n=8) and two independent cohorts of littermate Ube3a1x (untagged) mice (n=12 [saline], 14[PTZ]). **k**, Following seizures (above), qRT-PCR for *Cbln1* and *Ube3a* mRNA in, p-Ube3a^{mKO} (n=5), m-Ube3a^{mKO} (9) and WT (7/group), and, Ube3a1x (untagged, n=8/group). Mean ± SEM plotted.

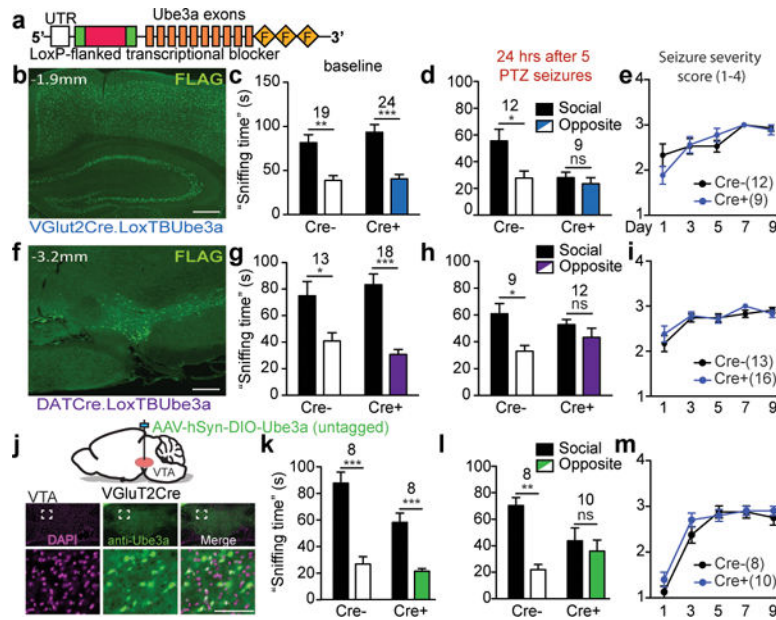


Figure 3. UBE3A-seizure synergy localizes to VTA

a, “LoxTB $Ube3a$ ” schematic. **b**, FLAG immunofluorescence in VGlut2Cre.LoxTB $Ube3a$ (cortex/hippocampus, scale bar: 400 μ m). **c**, Baseline sociability, **d**, post-seizure sociability, and **e**, seizure severity with subthreshold PTZ paradigm in LoxTB $Ube3a$ or VGlut2Cre.LoxTB- $Ube3a$. VGlut2Cre littermates. **f**, FLAG immunofluorescence in DATCre.LoxTB $Ube3a$ (midbrain, scale bar: 400 μ m). **g**, Baseline sociability, **h**, post-seizure sociability, and **i**, seizure severity with subthreshold PTZ paradigm in LoxTB $Ube3a$ or DATCre.LoxTB- $Ube3a$ littermates. **j**, Representative VTA-containing sections of VGlut2Cre. $Ube3a^{mKO}$ mice after injecting of AAV-hSyn-DIO- $Ube3a$, showing nuclear (pink, DAPI) and cytosolic UBE3A (green) in VTA (nuclear/UBE3A co-localized white; n=3 mice, scale bar: 100 μ m). **k**, Baseline sociability, **l**, post-seizure sociability, and **m**, seizure severity with subthreshold PTZ paradigm in VGlut2Cre or WT littermates 20d following VTA AAV-hSyn-DIO- $Ube3a$ injection. Mean \pm SEM plotted.

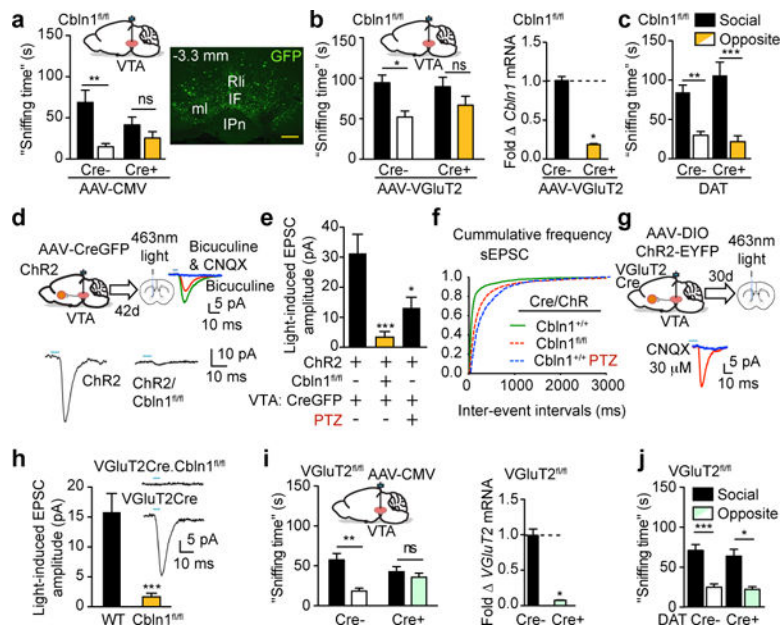


Figure 4. VTA *VGluT2*⁺ neuron-targeted deletions of *Cbln1* impair sociability and VTA-NAc glutamatergic synaptic transmission

a, Sociability in *Cbln1^{fl/fl}* mice with AAV-GFP (n=8) and AAV-CreGFP (n=12) injected into VTA and representative VTA-containing section showing GFP staining (RLi: rostral linear nucleus, IF: interfascicular nucleus, ml: medial lemniscus, IPn: interpeduncular nucleus). **b**, LEFT: Sociability following injections of AAV-VGluT2-RFP (n=13) or AAV-VGluT2-Cre-RFP (n=11) and RIGHT: qRT-PCR for VTA *Cbln1* mRNA (n=8). **c**, Sociability in *Cre-* (n=9) and *DAT-Cre+* *Cbln1^{fl/fl}* mice (n=6). **d**, Representative light evoked EPSCs from NAc medial shell MSNs with or without local *Cbln1* deletion. **e**, EPSC amplitudes for controls (n=12 neurons, 6 mice), following *Cbln1* deletion (n=15 neurons, 8 mice) or following PTZ exposure (n=10 neurons, 3 mice). **f**, Cumulative frequency plots of spontaneous EPSCs from neurons in **e**. **g**, Light-evoked VTA-NAc medial shell MSN EPSCs with AAV-hSyn-DIO-ChR2-EYFP in VTA of *VGluT2Cre* (n=14 neurons, 6 mice) or *VGluT2Cre.Cbln1^{fl/fl}* (n=22 neurons, 7 mice). **h**, LEFT: Sociability in *VGluT2^{fl/fl}* mice with VTA AAV-GFP (n=8) or AAV-CreGFP (n=12) and RIGHT: qRT-PCR for VTA *VGluT2* mRNA in **h**. **i**, Sociability in *Cre-* (n=11) or *DATCre+* *VGluT2^{fl/fl}* mice (n=6). Mean \pm SEM plotted.

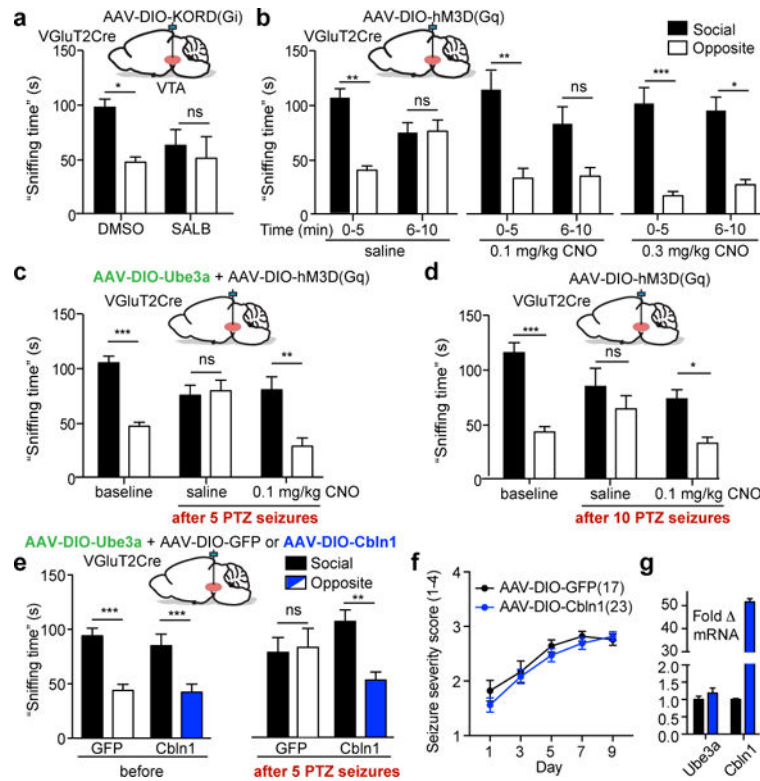


Figure 5. Sociability deficits produced by *Ube3a*-seizure synergy are rescued by chemogenetic activation or increased *Cbln1* mRNA in VTA *VGlut2* neurons

a, Sociability in VTA AAV-DIO-KORD injections in *VGlut2Cre* mice receiving either DMSO or SALB (10 mg/kg, s.c., n=13). **b**, Sociability (first and second 5 minute period of social trial) for VTA AAV-DIO-hM3D(Gq)-mCherry in *VGlut2Cre* mice (n=14). **c**, Sociability in VTA AAV-hSyn-DIO-Ube3a and AAV-DIO-hM3D(Gq)-mCherry co-injected in *VGlut2Cre* mice at baseline and after 5 PTZ-induced seizures comparing saline and CNO (n=18). **d**, Sociability for VTA AAV-DIO-hM3D(Gq)-mCherry injected *VGlut2Cre* mice at baseline and after 10 PTZ-induced seizures (n=16). **e**, Sociability before (LEFT, n=14[GFP], n=14[Cbln1]) and after (RIGHT, n=16[GFP], n=23[Cbln1]) 5 PTZ-induced seizures, **f**, seizure severity scores, and **g**, qRT-PCR validation (n=10/group) of VTA AAV-DIO-Ube3a/AAV-DIO-GFP or AAV-DIO-Ube3a/AAV-DIO-Cbln1 in VTA of *VGlut2Cre* mice. Mean \pm SEM plotted.